2021

Consensus Based Control Strategy for Virtual Synchronous Generators in Microgrids

Anusha kandula
West Virginia University, ak0099@mix.wvu.edu

Consensus Based Control Strategy for Virtual Synchronous Generators in Microgrids

Anusha Kandula

Thesis submitted
to the Benjamin M. Statler College of Engineering and Mineral Resources
at West Virginia University

in partial fulfillment of the requirements for the degree of

Master of Science
in
Electrical Engineering

Sarika Khushalani Solanki, Ph.D., Chair
Jignesh Solanki, Ph.D.
Muhammad A. Choudhry, Ph.D.

Lane Department of Computer Science and Electrical Engineering

Morgantown, West Virginia
2021

Keywords: Synchronverters, Virtual synchronous generator (VSG), Consensus Based Control,Virtual Inertia, Microgrids.

ABSTRACT

Consensus based Control Strategy for Virtual Synchronous Generators in Microgrids

Anusha Kandula

Renewable energy sources such as photo-voltaic and wind energy are integrating very rapidly in power systems. These energy-based systems typically adopt power-electronic interfaced inverters to connect to the grid. However, unlike traditional generators, these sources have low inertia, resulting in system stability issues, especially in microgrids where they are the primary sources. To mitigate the low-inertia effect, the inverters are modeled as virtual synchronous generators (VSG), and their control is designed. The VSG emulates the inertia effect of the synchronous generator and maintains the stability of the system. Even though the droop control provides the primary control, it is insufficient due to the high variability of the power electronics in inverter systems. Hence, optimal and efficient power-sharing among distributed generators (DGs) is needed through secondary control. The consensus- based algorithm is proposed in this thesis to overcome the control challenges of inverters in a microgrid to obtain control under fast-changing system conditions and unbalanced scenarios. The developed controller is tested on microgrid systems through simulations in MATLAB/Simulink, and the performance is compared with other controllers and with just the primary controller.

ACKNOWLEDGEMENT

I would like to express my profound gratitude towards many individuals, without kind support, it would not be possible for me to complete this master's journey.

I would like to express my deep and sincere gratitude to my advisor Dr. Sarika Solanki for accepting me as her master's student. Without her trust and support, encouragement and valuable guidance, this research would not have completed. Her dynamism, vision and motivation have deeply inspired me. Her methodology to carry out the research and present in it clear manner helped me achieve success. It was a great privilege and honor to work and study under her guidance.

I also would like to thank my co-advisor Dr. Jignesh Solanki for his valuable feedback throughout my research. His expertise in power systems helped me to finish this research. I would like to express my gratitude to Dr. Muhammad A. Choudhry, for being a part of my committee and providing the valuable feedback and suggestions which helped me improve my research. I also want to thank the Lane Department of Computer Science and Electrical Engineering for supporting me as a graduate student.

I made very good friends in this journey even a friend for life Sruthi Keerthi Valicharla, thank you for your support. I wish to specially thank all my lab mates and friends Vishal Verma, Deepak Tiwari, Mohammad Reza Khalghani, Hasan Ul Banna, who taught me lot of things technically and morally with their life experiences to make my journey at WVU smooth and joyful. Thank you for the continuous help and support.

I would like to thank my entire family: especially my grandfather who taught me value of education from my childhood and parents and in-laws for believing in me, my sister in-law, and my brother for their unconditional love and support throughout my journey.

Last but foremost, from the bottom of heart I would thank my husband Ravi Rayabarapu, for standing up for me and supporting me. I would never have made this step without him.

TABLE OF CONTENTS

LIST OF FIGURES

LIST OF TABLES

CHAPTER 1

Introduction

Smart grids are reliable and secure electricity infrastructures that can meet the future demand for transmission and distribution systems. Especially automation of distribution systems in smart grids welcomed the concept of microgrids. A microgrid is a part of a smart grid that is controllable and capable of supplying its own local load in isolation from mainstream power systems, called the islanded mode of operation [1]. Despite the ease associated with microgrids, there are many control and stability challenges. The complexity of the challenge increases with the energy sources in the microgrid. These energy sources are called distributed generators (DGs). Typically, these DGs are renewable power sources, such as solar, wind, biomass, and geothermal. Growing concerns about environmental injuries have led to an increase in these renewable energy sources. According to the United States Electrical Power Annual 2018, by 2024, the renewable fuel source increases by 23.1% [2]. However, these forms of energy are highly variable and need a sophisticated control system to maintain grid stability.

1.1 Literature Review

A distributed generator uses power-electronic interface converters called as Direct interfacing converters (DIC) to convert the energy into ac power. Compared to the traditional synchronous generator with rotor inertia (kinetic energy) and damping properties playing a significant role in maintaining the grid stability, DIC lacks these properties in the system [3]. Therefore, to possess these properties in DICs, droop control-based inverters mimicked properties of droop characteristics and maintain the system's stability was proposed in [4]. Although these droop control techniques enhance the system stability, the inertia of the grid is still an issue with highly variable renewable sources in the power systems. Because of this low inertia, the inverter's control needs to resemble a synchronous generator operation. This lead to the introduction of the concept of virtual inertia. These DICs with virtual inertia can be implemented in several ways, such as synchronverters, virtual synchronous machines (VSM), virtual oscillators, virtual synchronous generators (VSG). The concept of VSGs is to embed the complete characteristics of a traditional synchronous gener-

ator [5]. The conventional synchronous generator's inertial response and damping properties are obtained by implementing the swing equation—the dc source in the schematic acts as the power reserve of the kinetic energy. Over the past few years, the concept of this virtual inertia has been improvised in many ways [6–10]. The fundamentals, working concepts, and applications of VSG are demonstrated in [11]. [12] explained the idea of VSG with cascading of voltage and current loops, calling it a virtual synchronous machine, and performed the small-signal analysis of the VSM model, making the model easy to study the control and stability of the system. [13] improved the model to compensate for the coupling effect of VSG to the grid. [14] used the VSG as a battery storage system to enhance the islanded mode of operation. In [15], a comparison of droop-based inverters to VSG inverters in a microgrid was demonstrated. The discussion on the parallel operation of VSGs is mentioned in [16] and [17].

1.1.1 Secondary Control

The above research work of mimicking a conventional synchronous generator's dynamic characteristics helped to stabilize the output frequency and voltage. However, when operated in a multi-agent system, overall active and reactive power distribution is not satisfactory because of the static error of VSG especially during an unexpected load shifting. Given that VSG is also an inverter-based generator, the transient tolerance condition is much less than the synchronous generator. Consequently, VSG stops responding due to high oscillation caused by unexpected load shifting. The hierarchical secondary control of VSGs can address the issues in the primary control. The hierarchical structures are used conventionally in our power system. The secondary control mechanism of hierarchical structure improves the overall control and system stability. For example, [18] proposed a Bang-bang control strategy. In [19], the master-slave approach enhances stability. But the distribution of power among the DG's was not satisfactory because master-slave control is centralized control. Hierarchical control of VSGs maintained the power-sharing in [20], but practical feasibility was an issue because of small-signal analysis. [21] implemented the secondary control with a novel communication-less control method and achieved reactive power-sharing, but the dynamic response is not significant. Even though we adopt secondary control of VSG, we must consider the distortion created by the R/X ratio of the line impedances [22]. Reactive power-sharing in the system is affected by these line impedances. Additionally, consideration of single-point failures in the centralized control system is not suitable for robust microgrid control. A sophisticated control mechanism like consensus algorithm-based control is required to overcome this difficulty.

1.1.2 Consensus Algorithm

A consensus-based multi-agent control algorithm is employed in various studies like mobile networks convergence in multi-agent and many other applications like wireless sensor networking and coordination of multiple air crafts in recent studies. These algorithms are adopted for innovative grid applications for voltage support, economic dispatch, robust power-sharing, and multi-vehicle cooperative control [23]. The consensus algorithm uses the general agreement among all the agents to consider the entire network's desirable states. Communication interaction between neighboring agents and reliability over communication and switching delays enhance the parallel operation of multi-agent. Consensus-based distributed control on DIC was studied in recent years [24]. Given the precedence of distributed control over centralized control and to mitigate the static error of VSG, a consensus-based algorithm of VSG was implemented. Thus, microgrid stability and autonomous power-sharing can be achieved.

1.2 Thesis Objectives

- This thesis aims to deal with modeling of synchronous generators and its linearized models.
- To mimic the swing equation of a synchronous generator without the rotating parts as a VSG concept to provide advantages offered by a synchronous generator in grid stability.
- To analyze the different control topologies and their outcomes.
- To implement the consensus-based algorithm for the proper sharing of loads among individual generators.
- To study the effects of the R/X ratio of line impedances in the microgrid system.
- To investigate sensitives of implemented microgrid system with gain change of the consensus-VSG controller, and the effect of load change on the proposed controller.

1.3 Outline of Thesis

Chapter of the thesis are organized as follows:

- Chapter-2 covers the fundamentals network equations for microgrid components.
- Chapter-3 presents the concept of the virtual inertia and its classification.
- Chapter-4 presents the control and power-sharing between the inverters.

- Chapter-5 explains the proposed consensus-based control of the virtual synchronous generator and the simulation results.
- Chapter-6 summarizes the complete thesis, discusses the efficacy of consensus-based algorithms, and presents future work.

1.4 Summary

Power-sharing and stability of microgrid still raise concerns with the conventional controls as renewable DGs increases in the system. However, the consensus-based algorithm has previously been most influential in various fields to achieve the desired result. Therefore, modeling a microgrid with the consensus-based VSGs for power-sharing among all the generators is modeled in this thesis.

CHAPTER 2

Network equations of microgrid component

2.1 Introduction

Power systems structure are three-phase AC-systems comprising of generation, transmission and distribution systems. The transmission system is balanced three phase system that effectively distributes to single-phase and three-phase loads. The power produced by synchronous generators through conversion mechanical energy from primary sources (nuclear, hydraulic, and fossil). The generated power is transmitted to the end-users by the transmission system, with its subsystems operating at different voltages. From a control theory point of view, a power system is a high-dimensional complex system operating in a frequently changing environment. Several levels of control complexities are involved in supplying quality power to the end-users without any service disruptions. To design these controller a detailed representation of the system is needed. Figure 2.1 represents the control associated with a generating unit for maintaining stability of the system. The supplementary control adjusts the generator operating point according to the designed of control outcome.

2.2 Synchronous Generator model

Synchronous generators are the primary electrical sources in power systems. The grid stability depends on these generators, and thus, synchronism between the generators should be maintained for the stability of the system, which are in their dependent on rotor dynamics and the power-angle of the generator. Stability analysis requires Mathematical modeling of electromagnetic dynamics of a synchronous generator associated with its voltage and flux linkages.The electromagnetic dynamic equations are expressed in abc frame and can be simplified by Parks transformation to $dq-$reference frame. The significance of this reference frame is that it operates at nominal speed in steady-state conditions which makes it possible to represent quantities as time- invariant vectors. These vector quantities are related by swing equation discussed in next chapters. In this chapter we model synchronous generators, lines, loads and voltage source converters associated with newer

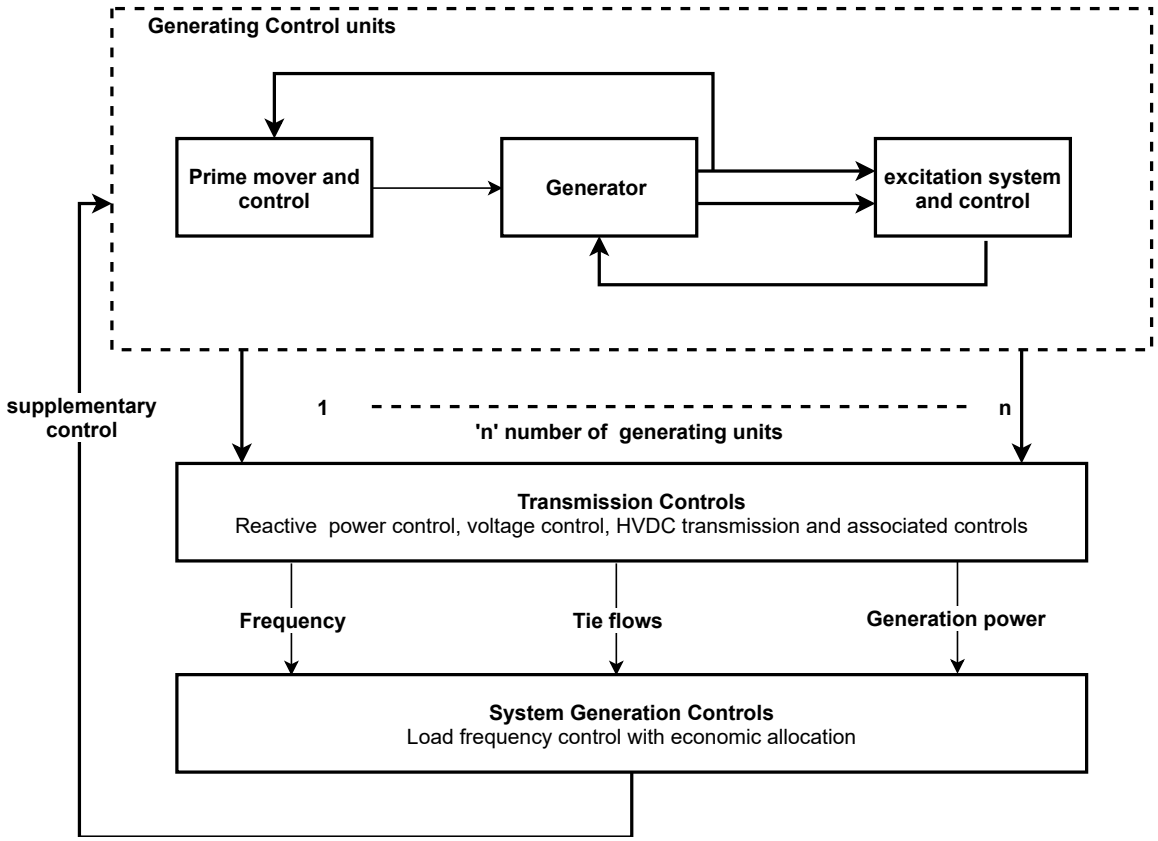

Fig. 2.1 Sub system of a power system and associated control

generating resources. These models are useful for designing supplementary controllers.

2.2.1 Rotor swing equation

The swing equation of synchronous generator can be written by considering Newton's second law of rotating mass states that the acceleration speed is proportional to the torqued resulted in 2.1:

$$J\frac{d\omega}{dt} = T_m - T_e \tag{2.1}$$

which is famously known as Swing equation [25][4][26]. Here J is the rotor inertia ($kg - m^2$), ω is the rotating speed (rad/sec). T_m is the mechanical torque generated by the prime mover, and T_e is the electromagnetic torque generated by EMF. For two-pole synchronous generator, the mechanical speed ω_m and electric speed ω_e are the same, i.e., $\omega_m = \omega_e = \omega$, and hence equation

2.1 can be rewritten in terms of mechanical power P_m, and electrical power P_e as:

$$J\frac{d\omega}{dt} = \frac{P_m}{\omega} - \frac{P_e}{\omega} \tag{2.2}$$

where $T_m = \frac{P_m}{\omega}$ and $T_e = \frac{P_e}{\omega}$ Considering mechanical friction in the system, which is proportional to the speed ω, equation 2.3 represents swing equation in terms of mechanical friction and speed.

$$J\omega\frac{d\omega}{dt} = \bar{P_m} - P_e - 2k\omega_o\Delta\omega \tag{2.3}$$

where $\bar{P_m} = P_m - k\omega_o^2$. Equation 2.3 can be represented in a per-unit system using a power base of S_b in 2.4.

$$\frac{J\omega_o}{S_b}\frac{d\omega}{dt} = \bar{P_m^{pu}} - \bar{P_e^{pu}} - \frac{2k\omega_o}{S_b}\Delta\omega \tag{2.4}$$

$$2H\frac{d\omega}{dt} = P_m - P_e - D_1\Delta\omega \tag{2.5}$$

the synchronous reference frame is δ and is related to the rotor position θ, where $P_e = \frac{EV}{X}sin\delta$,

2.2.2 Electrical Power and Torque

Electrical power in dq reference frames can be expressed as

$$P_e = v_d i_d + v_q i_q \tag{2.6}$$

And mechanical power can be expressed as

$$M_e = i_q\Phi_d + i_d\Phi_q \tag{2.7}$$

Electrical power can be expressed in terms of flux linkages as

$$P_e = (i_d\dot{\Phi}_d + i_q\dot{\Phi}_q) + (i_q\Phi_d + i_d\Phi_q)\omega - r(i_d^2 + i_q^2) \tag{2.8}$$

The flux linkages in equations 2.12 and 2.10 can be expressed as

$$\dot{\Phi}_d = -\frac{r}{l_d}\Phi_d + \frac{r}{l_d}\Phi_{AD} - \omega\Phi_q - v_d \tag{2.9}$$

$$\dot{\Phi}_D = -\frac{r_D}{l_D}\Phi_D + \frac{r_D}{l_D}\Phi_{AD} \tag{2.10}$$

$$\dot{\Phi}_q = -\frac{r}{l_q}\Phi_q + \frac{r}{l_q}\Phi_{AQ} - \omega\Phi_d - v_q \tag{2.11}$$

$$\dot{\Phi}_Q = -\frac{r_Q}{l_Q}\Phi_Q + \frac{r_Q}{l_Q}\Phi_{AQ} \tag{2.12}$$

2.3 Line Equations

From ith line connected between nodes j and k can be modeled in dq reference frame as

$$\frac{di_{lDi}}{dt} = \frac{-r_{li}}{L_{li}} i_{lDi} + \omega i_{lQi} + \frac{1}{L_{li}} v_{bDj} - \frac{1}{L_{li}} v_{bDk} \tag{2.13}$$

$$\frac{di_{lQi}}{dt} = \frac{-r_{li}}{L_{li}} i_{lQi} - \omega i_{lDi} + \frac{1}{L_{li}} v_{bQj} - \frac{1}{L_{li}} v_{bQk} \tag{2.14}$$

2.4 Load Equations

The load connected at ith node can be modeled as

$$\frac{di_{loadDi}}{dt} = \frac{-R_{loadi}}{L_{loadi}} i_{loadDi} + \omega i_{loadQi} + \frac{1}{L_{loadi}} v_{bDi} \tag{2.15}$$

$$\frac{di_{loadQi}}{dt} = \frac{-R_{loadi}}{L_{loadi}} i_{loadQi} + \omega i_{loadDi} + \frac{1}{L_{loadi}} v_{bQi} \tag{2.16}$$

2.5 Voltage Source Control (VSC)

A voltage source converter (VSC) is crucial in a microgrid to interface distributed energy sources to the power grid. Modeling of VSCs comprises of mathematical representations for power, voltage, current controller dynamics, output filter dynamics, and coupling inductor dynamics. Modeling of VSCs allows designing of controllers for frequency and voltage. This section develops linear models for voltage source converter considering all its control modes.

2.5.1 Inner current loop

A VSC is connected to the system at PCC through an RL circuit. Figure 2.2 shows VSC with its inner and outer control loops. The references for these loops are dependent on the models of VSC control and are discussed in this section. The dynamics of the circuit can be written in dq-axes

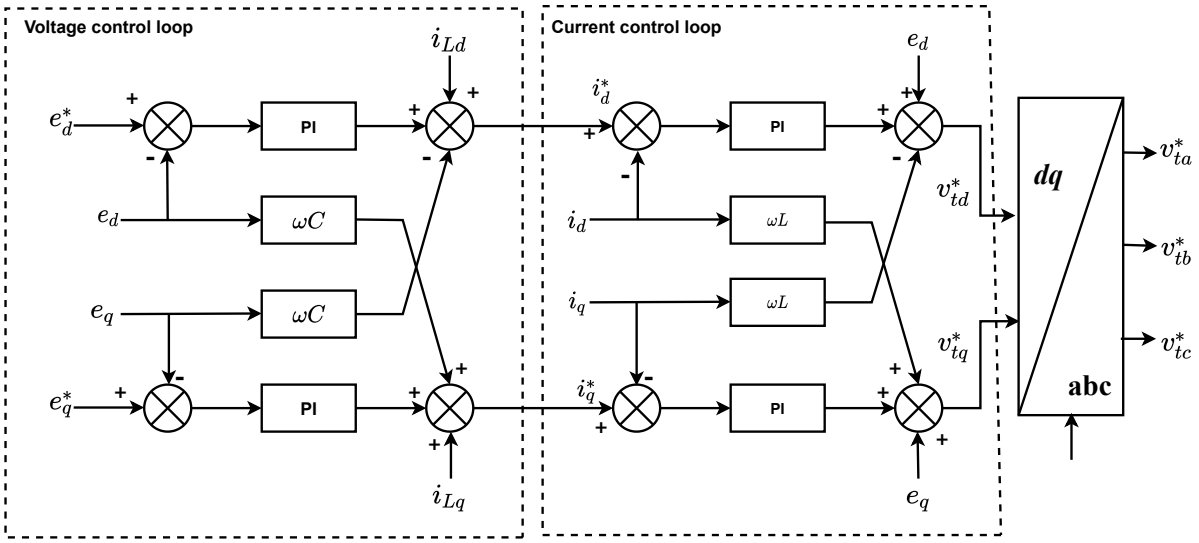

Fig. 2.2 Block diagram of VSC control

frame as in equation 2.17 where v_1 is the voltage at the PCC.

$$\begin{aligned} L\frac{di_d}{dt} + Ri_d &= \underbrace{v_d - v_{1d} + \omega L i_q}_{u_d} \\ L\frac{di_q}{dt} + Ri_d &= \underbrace{v_q - v_{1q} - \omega L i_q}_{u_q} \end{aligned} \tag{2.17}$$

u_d and u_q are the inputs of inner current control loop. Current i_d is compared with the reference current i_d^* and amplified to regulates the PCC voltage to reference voltages.

2.5.2 Phase Lock Loop (PLL)

As shown in Figure 2.2, input to pll phase voltages of the grid and output is the voltages in dq reference frame governed by equation 2.18. For this conversion θ_{PLL} is angle obtained from grid voltage.

$$\begin{aligned} v_d &= \frac{2}{3}\Big(v_a cos(\theta_{PLL}) + v_b cos\big(\theta_{PLL} - \frac{2\pi}{3}\big) + v_c cos\big(\theta_{PLL} + \frac{2\pi}{3}\big)\Big) \\ v_q &= -\frac{2}{3}\Big(v_a sin(\theta_{PLL}) + v_b sin\big(\theta_{PLL} - \frac{2\pi}{3}\big) + v_c sin\big(\theta_{PLL} + \frac{2\pi}{3}\big)\Big) \end{aligned} \tag{2.18}$$

2.5.3 Modes of VSC control

In any mode of operation the references are generated from equation $p = v_d i_d^* + v_q i_q^*$. In PQ control mode the power is maintained constant, in PV control mode power is obtained to maintain voltage constant, and in V_f control mode power is obtained to make frequency constant. There are two modes for VSC control namely PQ/PV and VF control depending on the islanded or non- islanded mode of microgrid opeation. The outer current loop dynamics are slower than the inner current loop to reflect the dynamic changes.In the pq control mode the references are obtained considering constant power. In VF mode the references are generated using equation 2.21 and in pq/pv mode references are generated using following equations.

$$\begin{aligned} C\frac{de_d}{dt} - \omega C e_q &= i_d - i_{Ld} \\ C\frac{de_q}{dt} + \omega C e_d &= i_q - i_{Lq} \end{aligned} \tag{2.19}$$

The plant model suitable for linear control system design is as follows:

$$\frac{e_q}{u_q} = \frac{e_d}{u_d} = \frac{1}{Cs} \tag{2.20}$$

where,

$$\begin{aligned} u_d &= i_d - i_{Ld} + \omega C e_q \\ u_q &= i_q - i_{Lq} - \omega C e_d \end{aligned} \tag{2.21}$$

In equation 2.21, u_d and u_q are the outputs of the PI controller, where reference currents i_d^* and i_q^* use the following relationships.

$$\begin{aligned} i_d^* \approx i_d &= u_d + i_{Ld} - \omega C e_q \\ i_q^* \approx i_q &= u_q + i_{Lq} + \omega C e_d \end{aligned} \tag{2.22}$$

2.6 Summary

In this chapter, electromechanical linearized dynamics of the synchronous generator, line, load and voltage source inverter are explained through the state-space model representation. This representation can be used for analyzing power voltage and frequency control in the system. The voltage source converters provide more controllability to the grid than synchronous generators because of the controllable parameters in their design. Furthermore, the VSC control strategy offers the flexibility to operate in either PQ or V-f mode. For simultaneous operation of inverters, these modes of operation have high power and voltage regulation performance for autonomous power-sharing. The power-sharing properties are explained in detail in Chapter 3.

CHAPTER 3

Modeling and Classification of inverters

3.1 Classification of inverter-based Distributed generators

Renewable energy sources and heavy loads in power distribution networks, such as EV charging stations, wind farms causes instability issues in the grid. In islanded mode of operation of a micro-grid, a control solution for stable operation of the grid can be achieved by proper power-sharing and control methods between the inverters. The converters can be classified based on whether they are controlled as grid forming or grid following inverters. Grid following inverters regulate their power output through the change in voltage angle which is measured using a phase-locked loop. Hence, they merely follow the grid angle/frequency and do not actively control their frequency output. In contrast, Grid-forming inverters actively control their frequency output using droop controlled method to support the system frequency under changing load conditions.

Grid-forming inverters can play a constructive role in improving inverter-dominated power system's frequency dynamics and stability. VSI(voltage source inverter) is an example of a low-inertia inverter that controls the grid voltage and frequency using droop control. The inverters can be classified further as shown in Figure 3.1 depending on their inertia characterstics. The governer controlled reference power generation adds inertia to the system just like a synchronous machine and hence it is called virtual synchronous generator (VSG). The rotor angle controlled reference power generation also adds inertia to the system just like a synchronous machine and hence it is called VSM. The torque controlled is called as synchronverters. In this section modeling of these inverters are explained in detail and control analysis is described in next chapters.

3.2 Non-inertia-based Droop inverters

Distributed energy resources use power electronic inverters as an interface to connect the grid. The traditional power systems are dominated by Synchronous Generators(SG). SG has well-defined controllers with dynamic characteristics such as inertia that control the change in speed of the rotor due under sudden disturbances. Traditional SG's controllability when operated in a wide

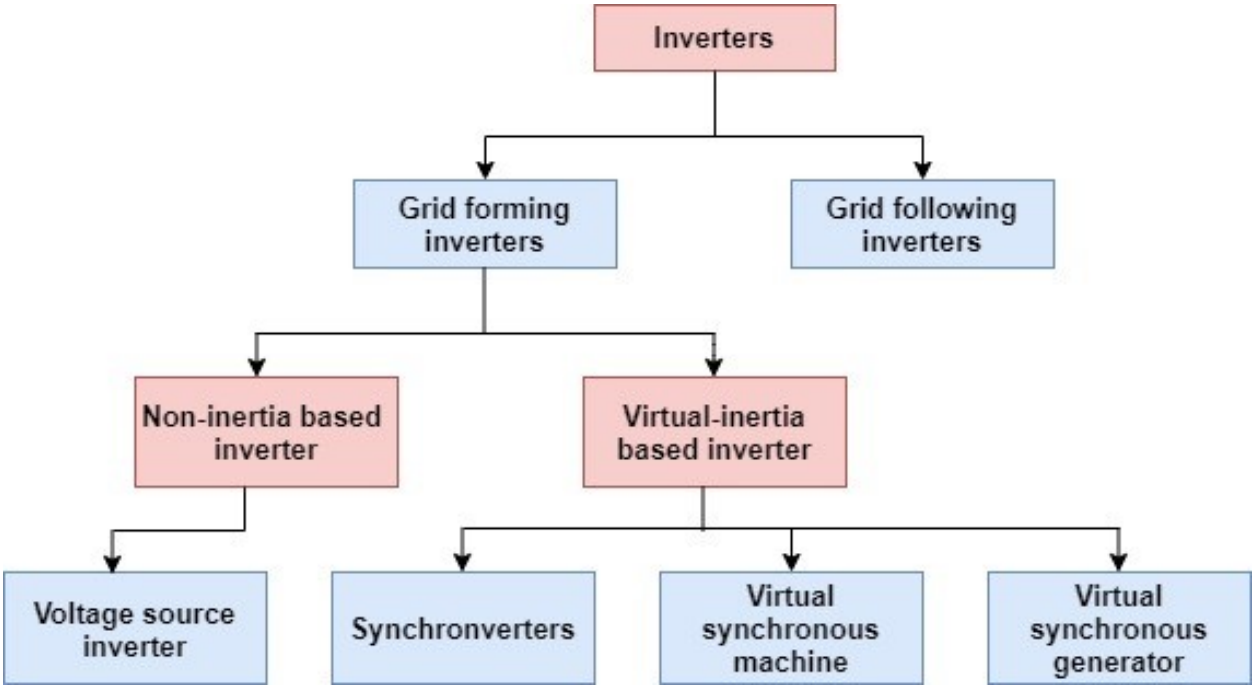

Fig. 3.1 Classification of interfacing inverters in the microgrid

range is challenging, due to its mechanical parts where as power inverters ease the controllability. Several researchers developed droop-based inverters to mimic the governor properties of the SG, which change the output frequency f according to the load change. The dynamics of the droop controllers of SG and droop inverters are developed as shown in equations 3.1 and 3.2.

In 3.1 the percent droop determines the change in frequency and is obtained by difference between no load and full load speed.

$$\%droop = \frac{No\ load\ speed\ of\ the\ generator\ \ -\ \ full\ load\ speed\ of\ the\ generator}{full\ load\ speed\ of\ the\ generator} \tag{3.1}$$

Droop controlled voltage source inverter uses the principle of speed change of synchronous generator active and reactive power change as equation 3.2.

$$\begin{aligned} f &= f_r - k_p(P_{ref} - P_s) \\ V &= V_r - k_v(Q_{ref} - Q_s) \end{aligned} \tag{3.2}$$

Here, f_r and V_r are the reference frequency and reference voltage of the system, respectively. P_s and Q_s are active and reactive power generated by the inverter. k_p and k_v are frequency and voltage droop gains, respectively. Even though voltage source inverters have some advantages, the limitations of output current create voltage instability in the system with a low short-circuit

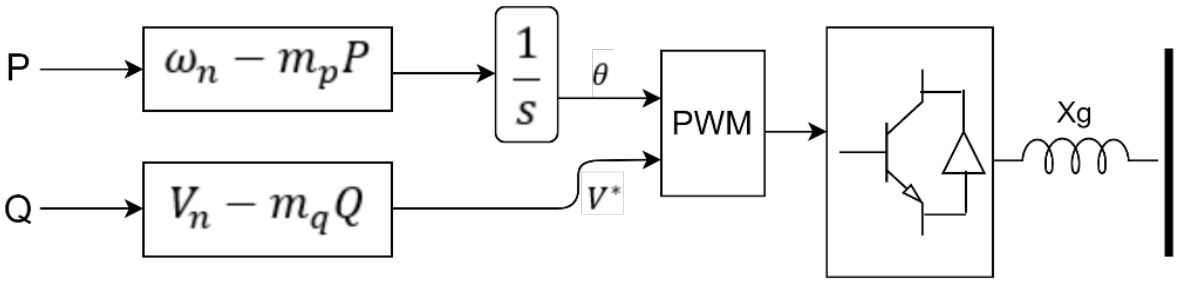

Fig. 3.2 Control block diagram of Droop-based inverter

capacity due to lack of inertia in the system.

3.3 Virtual inertia based inverters

According to the ERCOT (Electric Reliability Council of Texas) [28], In Nov 2018, the minimum inertia requirement of the Texas power system was about $129GW$, which was almost 30%more than system inertia (100 GW's) as shown in figure3.3. This effect does not allow the system to arrest the frequency above the low limit, which results in load shedding, followed by simultaneous loss of the two large generators in the system triggering off. The low-inertia effect was profound due to $13.5GW$ additional wind energy sources added between 2013-2019.

To overcome these issues, control of power inverters should replicate the control of conventional power generator (SG) dynamics using novel techniques. Parallel operation of these inverters is also possible for improved rating and higher inertia. To mimic a synchronous generator properly

ERCOT report for minimum inertia hour in each year							
Date and time	2013 3/10/13 3:00am	2014 3/30/14 3:00am	2015 11/25/15 2:00am	2016 4/10/16 2:00am	2017 10/27/17 4:00am	2018 11/03/18 3:30am	2019(jan-nov) 3/27/2019 1:am
Min.synch.Inertia (GW's)	132	135	152	143	130	128.8	134.5
System load at minimum synch.inertia(MW)	24,726	24,540	27,190	27,831	28,425	28,397	29,883
Non-synch,in percantage of system load	31	34	42	47	54	53	50

Fig. 3.3 ERCOT Inertia chart in each year from 2013-2019

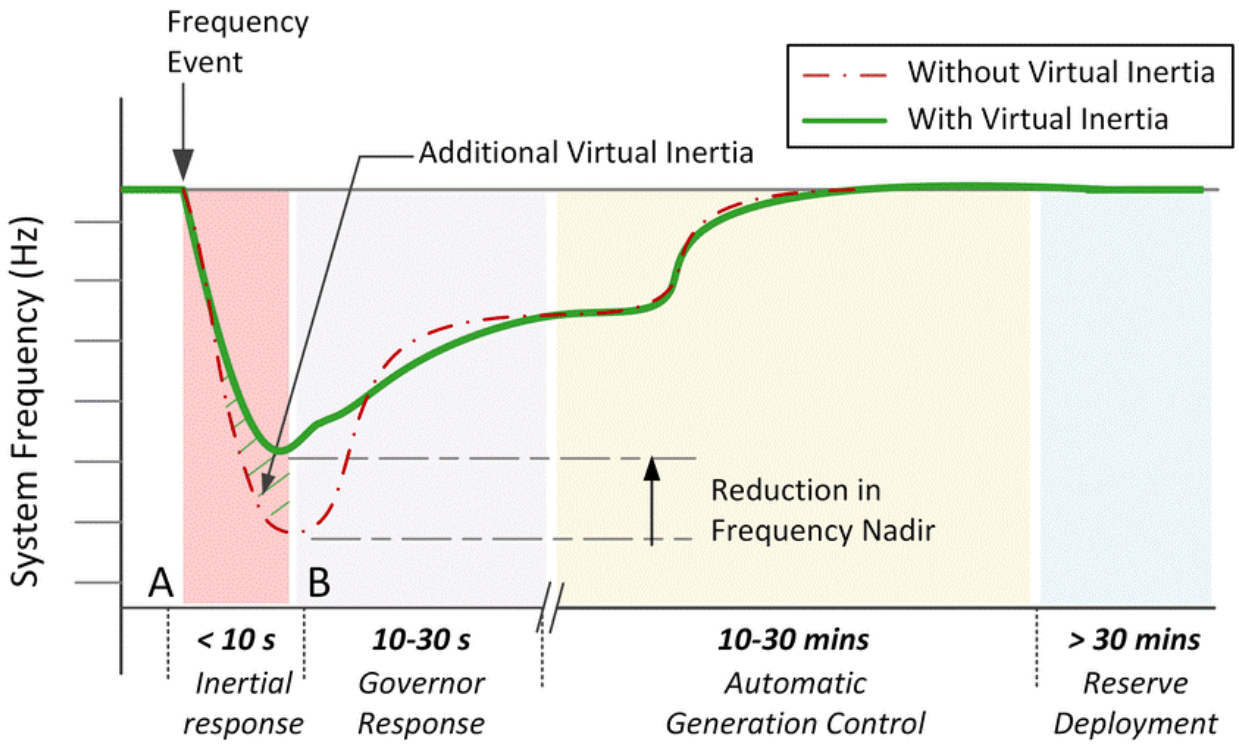

Fig. 3.4 Multiple time-frame frequency response in a power system following a frequency event

a detailed analysis of frequency event is needed as shown in the figure. 3.4 [27].

A generator load imbalances event trigger intial response first followed by governer and automatic generation control responses as shown in figure 3.4. When any disturbances occur, the generators cannot respond instantaneously as kinetic energy stored in the rotor acts as a counter-response to the disturbance until the primary frequency control is activated. As renewable energy sources replace the conventional generators, the rate of change of frequency increases due to low inertia of the system. The relationship of change in active power to change in frequency can be derived using equation 3.4 and replaced ω_g in 3.4 with $\frac{df}{dt}$.

$$P_{gen} - P_{load} = \frac{dE_{k.e}}{dt} = \frac{d}{dt}\left(\frac{1}{2}J\omega_g^2\right) = J\omega_g\frac{d\omega_g}{dt} \tag{3.3}$$

Where P_{gen} and P_{load} are the generated power and power demand with losses, respectively. J is the inertia of the system and ω_g is the system frequency, the inertia constant H of the power system is the kinetic energy normalized to apparent power S_g of the generators in the system. The equation 3.4 can be written in terms of frequency as follows:

$$\frac{2H}{f}\frac{df}{dt} = \frac{P_{gen} - P_{load}}{S_g} \tag{3.4}$$

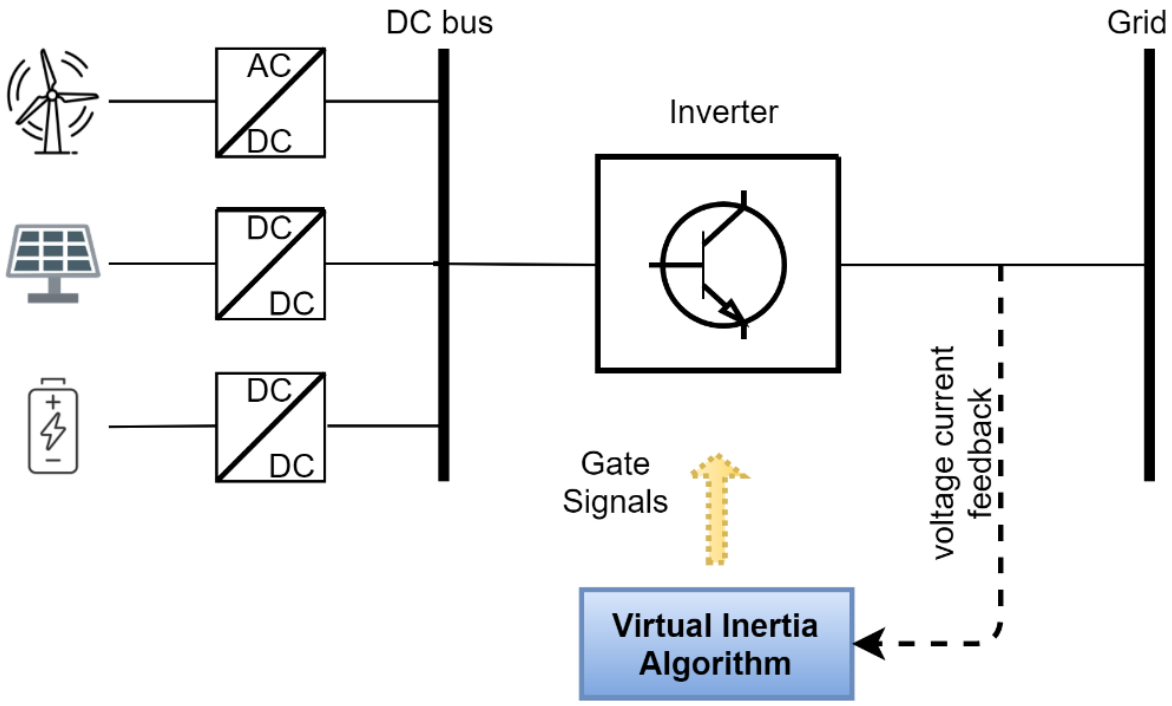

Fig. 3.5 Concept of virtual inertia

Where $\frac{df}{dt}$ is the rate of change of frequency. The system inertia plays an important factor when the microgrid is isolated than grid-connected due to limited energy sources. Therefore the implementation of virtual inertia is essential to the operation of power electronic converters as synchronous generators. Virtual inertia can be represented through combination of control algorithms, renewable energy sources, energy storage systems, and power electronics. Figure 3.5 shows the concept of virtual inertia and can be modeled based on the desired application and model sophistication. Three main topologies of virtual inertia based converters are discussed in the following sections.

3.3.1 Modeling of synchronverters

The synchronverters provide inertia, damping of oscillations, and regulate the bus voltage in the grid. Synchronverter gives seamless switching in MG, since synchronverter parameters are not fixed and can be adjusted according to the properties of the integrated network without any physical limitations. Since the synchronverter can synchronize with the grid, the synchronverter can work as a self-synchronized inverter without using PLL (Phase Lock Loop), a major non-linear element. This self-synchronization greatly assists in an improved system [30]. To model a self-synchronous converter an AC/DC converter that converts the DC voltage to the three-phase AC

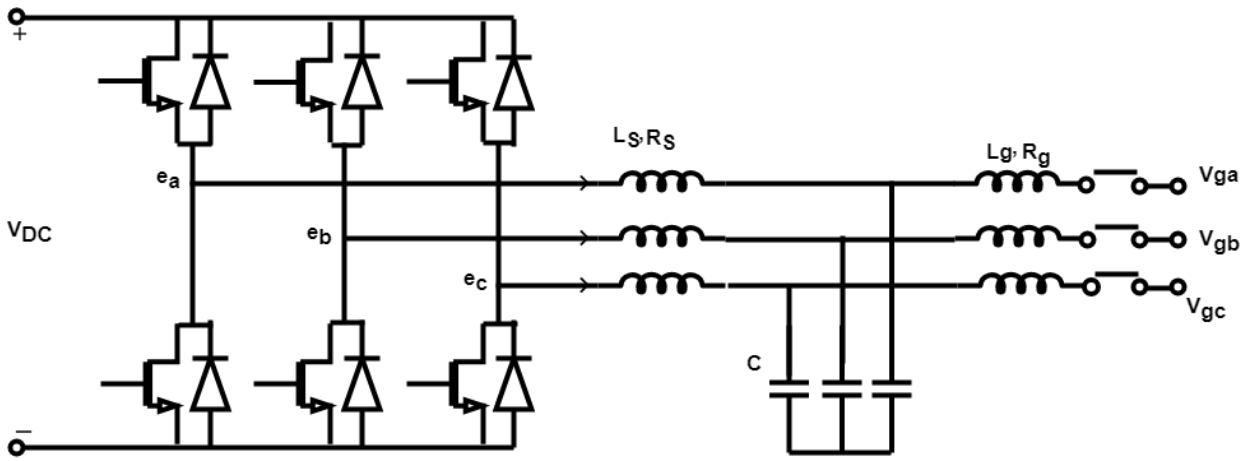

Fig. 3.6 Power part of Synchronverter

power is used and shown in Figure 3.6. Pulse Width Modulation (PWM) to generate switching sequence for inverter switches and LC filter is used to reduce ripples. In the grid-connected operation of synchronverter, the connection is through grid inductance and resistance (L_g and R_g respectively), as well as synchronverter resistance and inductance (L_s and R_s), filter capacitor, and circuit breaker. Generated voltage e (e_a, e_b, e_c) is the back emf and is represented in equation 3.5 where i_f is the output current and V_f is the terminal voltage of the system. M_f is maximum mutual inductance between stator winding and field winding, and θ is the virtual angular speed. Figure 3.7 shows the control mechanism of the sychronverter and is governed by the equations 3.6. where as the mechanical dynamics are modeled in equation 3.7.

$$e = \dot{\theta} M_f i_f sin\theta \tag{3.5}$$

$$\begin{aligned} P = T_e\dot{\theta} &=< i, e > \\ Q &=< i, e_q > \end{aligned} \tag{3.6}$$

Mechanical dynamics of synchronous generator are modeled in synchronverter as:

$$\begin{aligned} \ddot{\theta} &= \frac{1}{J}(T_m - T_e - D_p\dot{\theta}) \\ T_e &= M_f i_f < i, \tilde{sin}\theta > \end{aligned} \tag{3.7}$$

where T_m, T_e, θ, J, Q are the mechanical torque applied to the rotor, the virtual electrical torque, the rotor angle, the imaginary moment of inertia, and the reactive power, respectively.

The active power control is highly dependent on virtual mechanical friction coefficient D_p and is proportional to change in the torque acting on virtual rotor and inversely proportional to

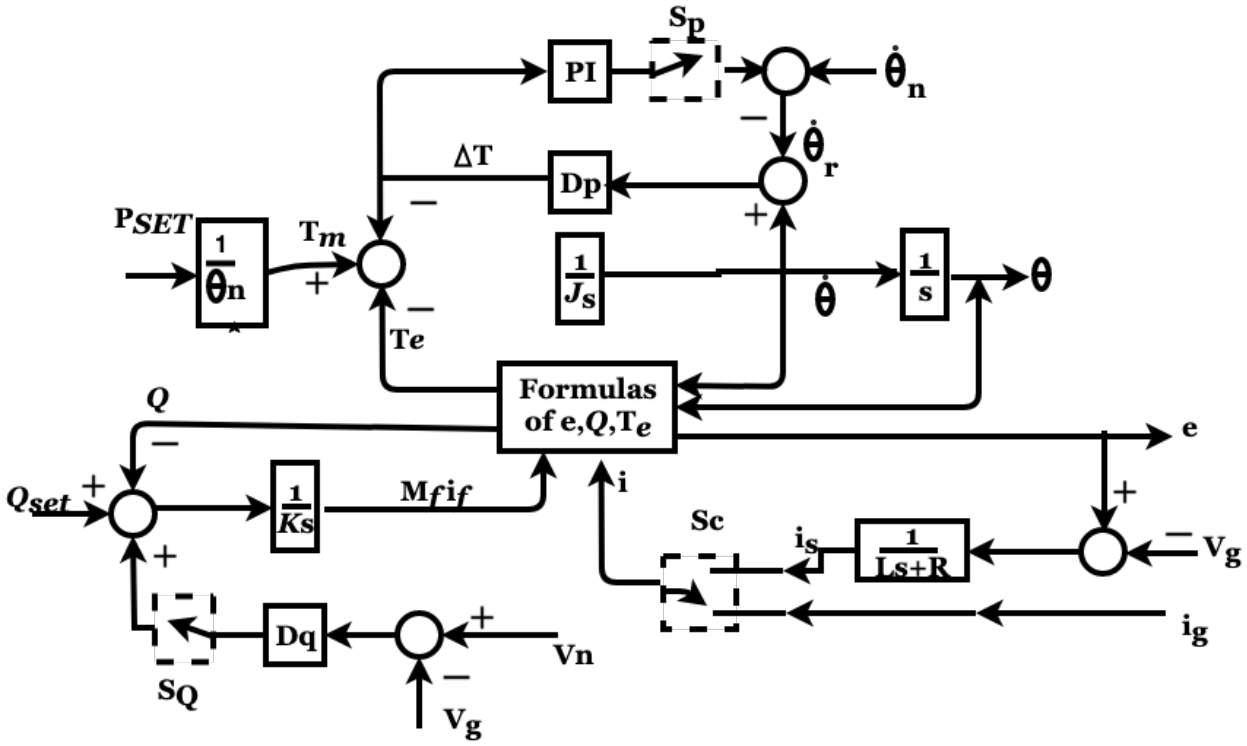

Fig. 3.7 Electronic part of Synchronverter

the angular frequency. In the same way, D_q controls the reactive loop and is proportional to the difference between the reference voltage and grid voltage and thus regulates the field excitation $M_f i_f$. In an islanded mode of operation, a PI controller is used to maintain the frequency and the virtual current i_s as shown in equation 3.8 flowing through the reactance (sL+R) of the inverter.

$$i_s = \frac{1}{sL + R}(e - v_g) \tag{3.8}$$

The virtual current is can be synchronized with the grid current i_g using S_p, S_Q switches. The controller for torquet_e and angular speed $omega$ are discussed in the section.

3.3.2 Modeling of a Virtual Synchronous Generator

The Virtual Synchronous Generator (VSG) is the governer controlled reference power generator based on frequency as shown in figure 3.8. VSG emulates the release or absorption of kinetic energy like SG through the DC-link energy storage in the topology.

The VSG control is represented by the swing equation in 3.9 and 3.10 [15].

$$P_{in} - P_{out} = J\omega_m \frac{d\omega_m}{dt} + DS_{base}\frac{\omega_m - \omega_g}{\omega_o} \tag{3.9}$$

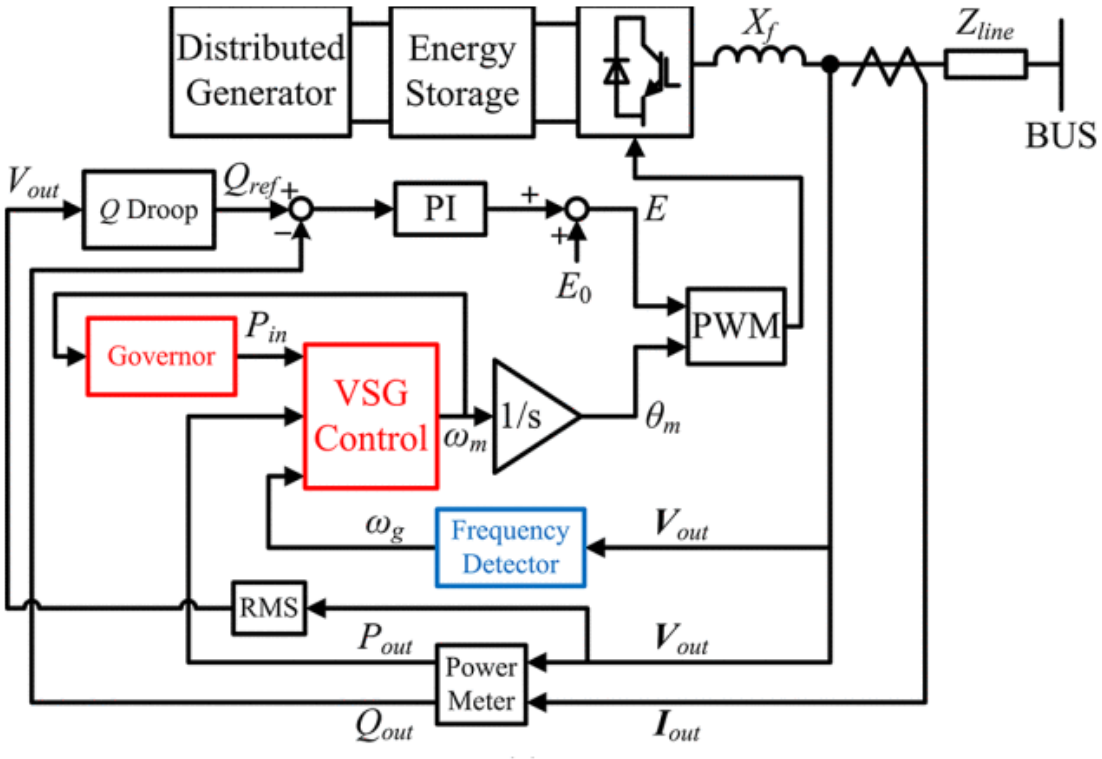

Fig. 3.8 Block diagram of virtual synchronous generator

$$P_{in} = P_o - k_p S_{base} \frac{\omega_m - \omega_g}{\omega_o} \tag{3.10}$$

Where P_{in} is the virtual shaft power determined by the governor,P_{out} is the measured output power, J is the virtual inertia, ω_m is the angular frequency of virtual rotor, S_{base} is the power rating of DG, $\omega_g$is the angular velocity at the voltage sensor and ω_o is the nominal frequency, P_o is the reference value of the active power and k_p is the droop coefficient. The swing and governor equations represent the control dynamics, and the resulting equation 3.11 is as follows:

$$P_o - P_{out} = J\omega_m \frac{d\omega_m}{dt} + D_p \frac{\omega_m - \omega_g}{\omega_o} + k_p(\omega_m - \omega_o) \tag{3.11}$$

where $k_p = k_p S_{base}/\omega_o$, $D = DS_{base}/\omega_o$. The control of VSG is explained in further chapters.

3.4 Summary

The stability and controllability of conventional power systems are not sufficient with the high-level penetration of renewable DGs. Therefore, the concept of investigating inverter dynamics was the approach to enhance the stability analysis of the microgrid system. These approaches lead to modeling of the droop-based inverters to attain the stability and controllability of the microgrid. However, due to the further increase in renewable energy sources like solar and wind energy, the droop-based inverters can not support the system demands entirely because of low inertia, so virtual inertia based inverters were modeled.

CHAPTER 4

Control of the inverters

4.1 Introduction

In this chapter, the control mechanism of inverters mentioned in the above chapters is described. Individual inverter mechanism represented sections. The parallel operation of droop-based inverters is compared with the parallel operation of the synchronverter. Comparsion of all three inverters is explained by summarizing the advantages and disadvantages. Finally, MATLAB simulation is used to verify the results.

4.2 Voltage Source Inverters in the islanded mode of operation

Consider two DGs both rated 10kVA with control parameters as shown in table sharing the load equally in islanded microgrid system. The DG's share the load according to the droop control strategy, as shown in Figure 3.2 in above chapter. As shown in figures 4.1 and 4.2, at t=1.4 seconds an additional load is added which is shared equally among the DGs. VSIs are faster and have more underdamped response following a load change. However, the fast response of VSIs in the case of faults may sometimes instability.

4.3 Synchronverter in grid connected and islanded mode

Synchronverter operates in different modes based on the status of switches S_p, S_Q, S_c. In the self synchronizing mode of synchronverter the switch S_c position 1, S_p is ON, S_Q is OFF, the real and reactive powers are zero. In the power mode of synchronverter the switch S_c is in position 2 and S_p is ON position and S_Q is OFF position, this mode of operation is called P-mode, produced power (P) tracks the reference power (P_ref). Similarly, when S_Q is ON, S_p is ON and S_c is in position 2, this mode is called Q-mode, and produced reactive power tracks the reactive reference power (Q_ref). Inductance L and resistance R are chosen such that even small changes in i_s will result in large transient currents in the controller allowing smooth tracking of reference power. The real and reactive power of synchronverter are shown in . Table 4.1 shows the control parameters and

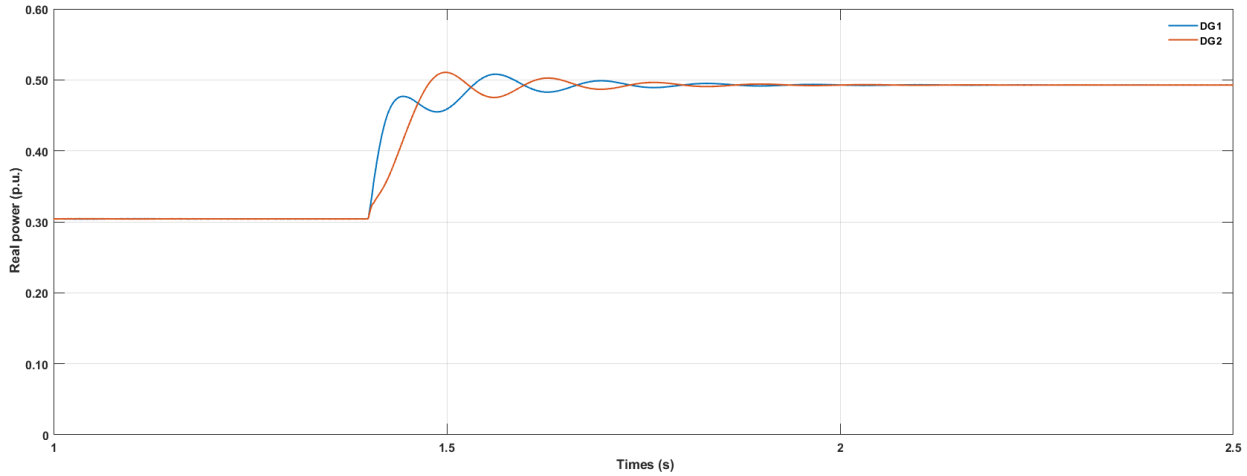

Fig. 4.1 Real power-sharing among the droop-based inverters

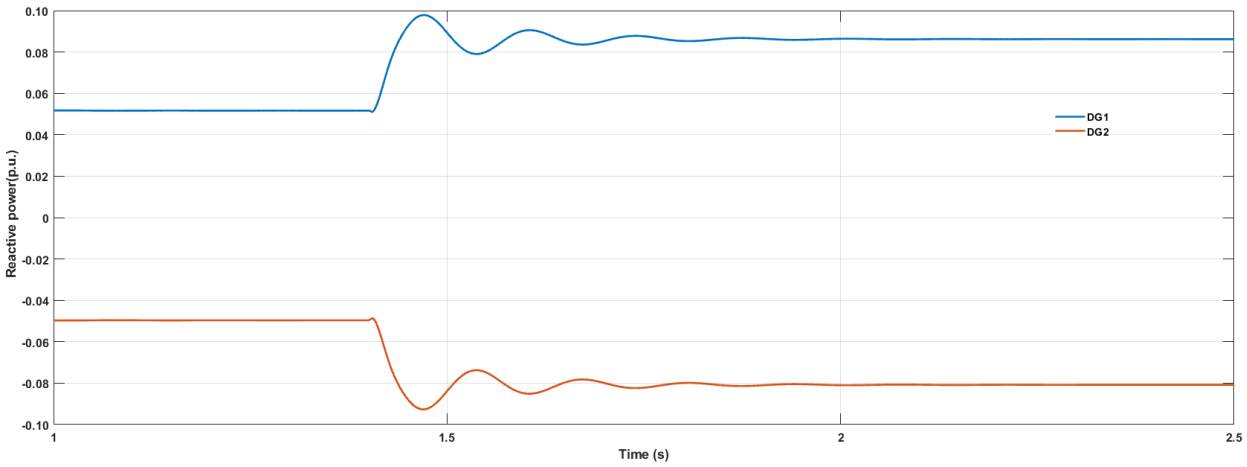

Fig. 4.2 Reactive power-sharing among droop-based inverters

variations of J and D_p affect the response in figures 4.3 and 4.4 respectively. The results for the islanded operation of synchronverter based inverters are compared with droop-based inverters. It is observed that in VSI, there are more oscillations in active and reactive power as compared to synchronverters for a load change. This shows that synchronverter response is superior over VSI response.

The islanded operation of synchronverters compared with that of VSI in figures 4.1 and 4.2. As shown in figures 4.3 and 4.4 at t=2seconds additional load is added and at t=4sec microgrid starts operating in islanded mode. It is seen that the synchronverter transitions to supply additional load as well as stand alone mode.

Table 4.1 System Parameters

parameters	values	parameters	values
R_s	0.135Ω	V_s	$12\sqrt{2}$
C	22μ F	dc-link	42
L_g	0.15mH	K_i	20
τ_f	0.002	τ_v	0.02
R_g	0.045	K_p	0.5

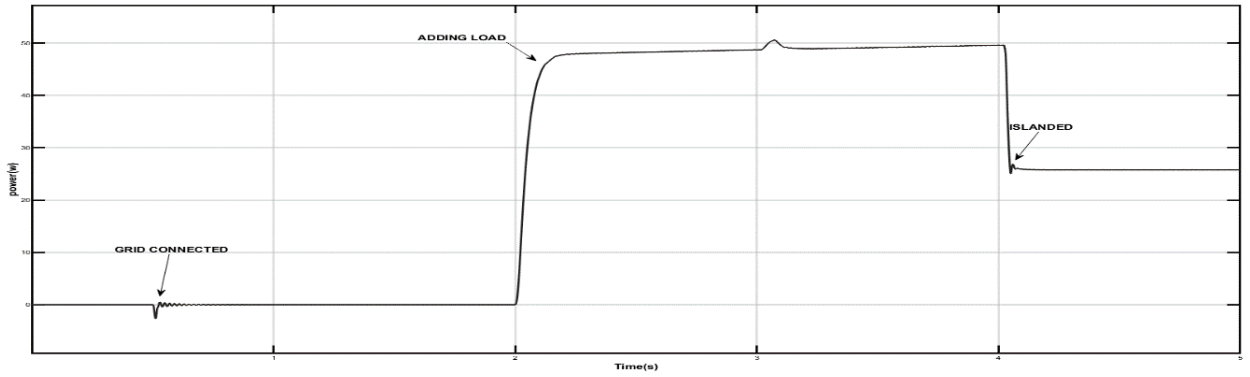

Fig. 4.3 Real power of the synchronverter

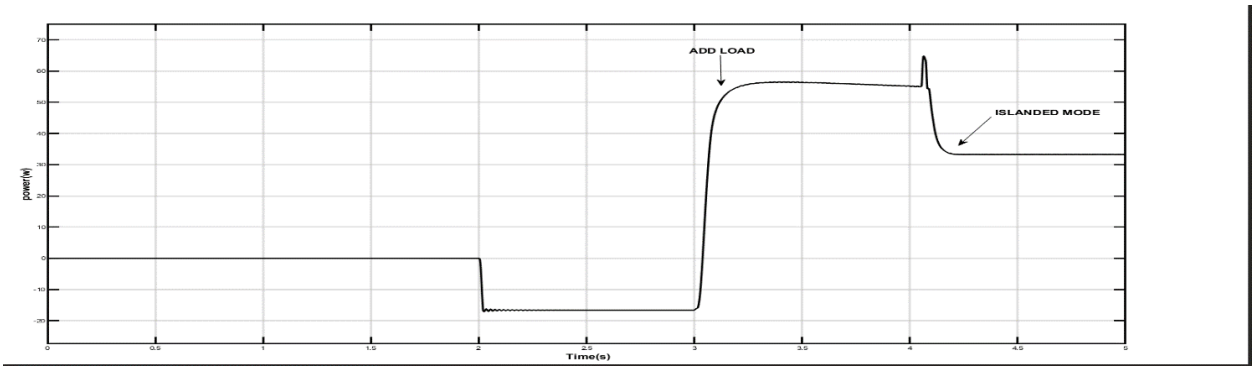

Fig. 4.4 Reactive power of the synchronverter

4.3.1 Parallel operation of synchronverters in grid-connected and islanded mode

Consider two synchronverters both rated 100 W, operating at 12 V and 14 V. Under normal operating conditions, the synchronverter is synchronized with the grid as discussed in section-4.3. As shown in figures 4.5 and 4.6, at t=2sec an additional load is added which is showed in accordance with the rating of the synchronverter. At t=4.5seconds the islanded mode of operation begins with load shedding to avoid overloading at first and t=5sec some of the load is restored. In the islanded mode of operation the reactive power doesnot track the reference ending up in a static effect. In

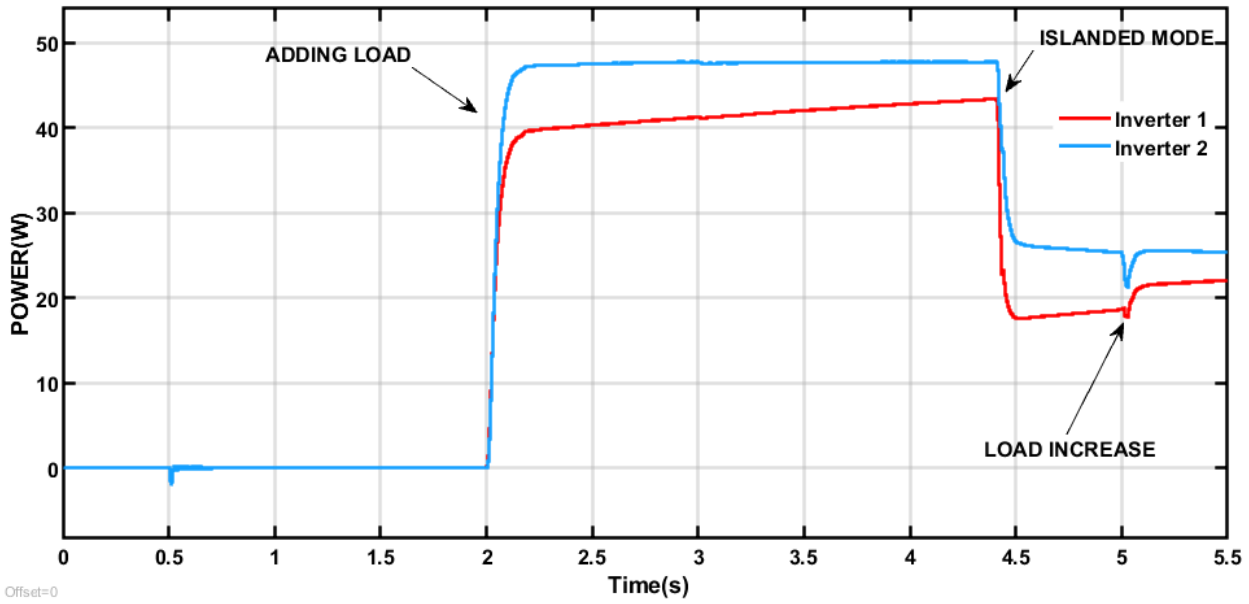

Fig. 4.5 Active power-sharing between the synchronverter

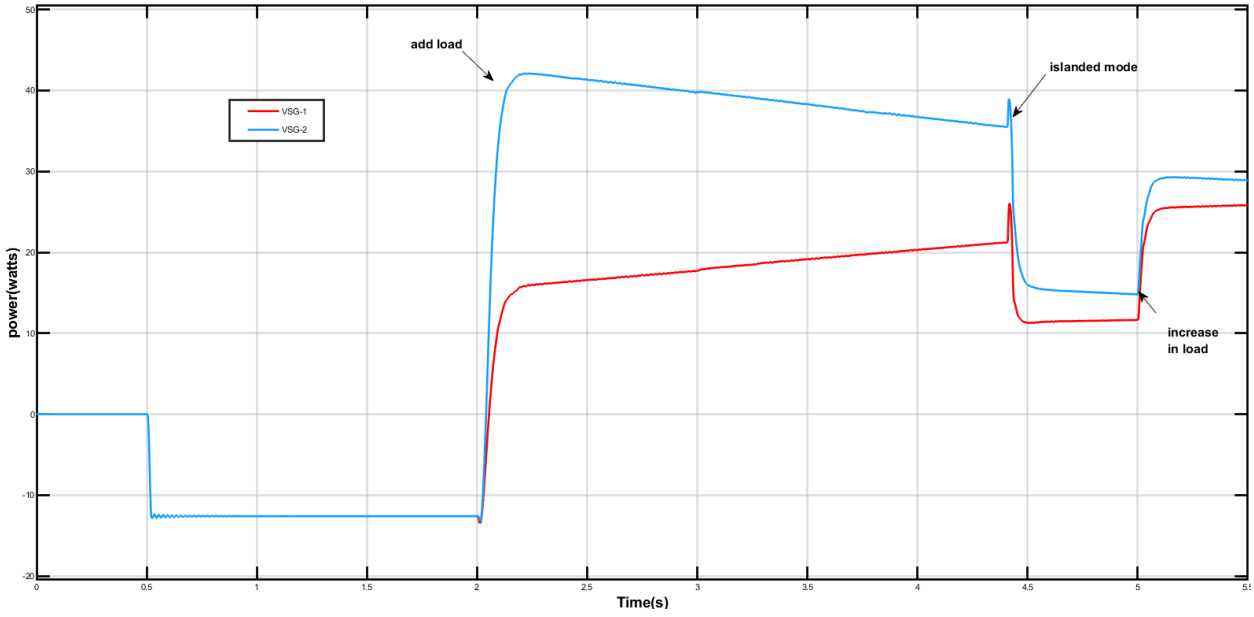

Fig. 4.6 Reactive power-sharing between the synchronverter

the next section a power doesnot track governor control introduced as shown in figure 3.8, which also adds an additional delay in the inverter.

Table 4.2 System Parameters

parameters	values	parameters	values
J	56.3 $kg.m^2$	D_p	$17pu$
ω_0	376.99$\frac{rad}{s}$	governor-time constant	$1sec$

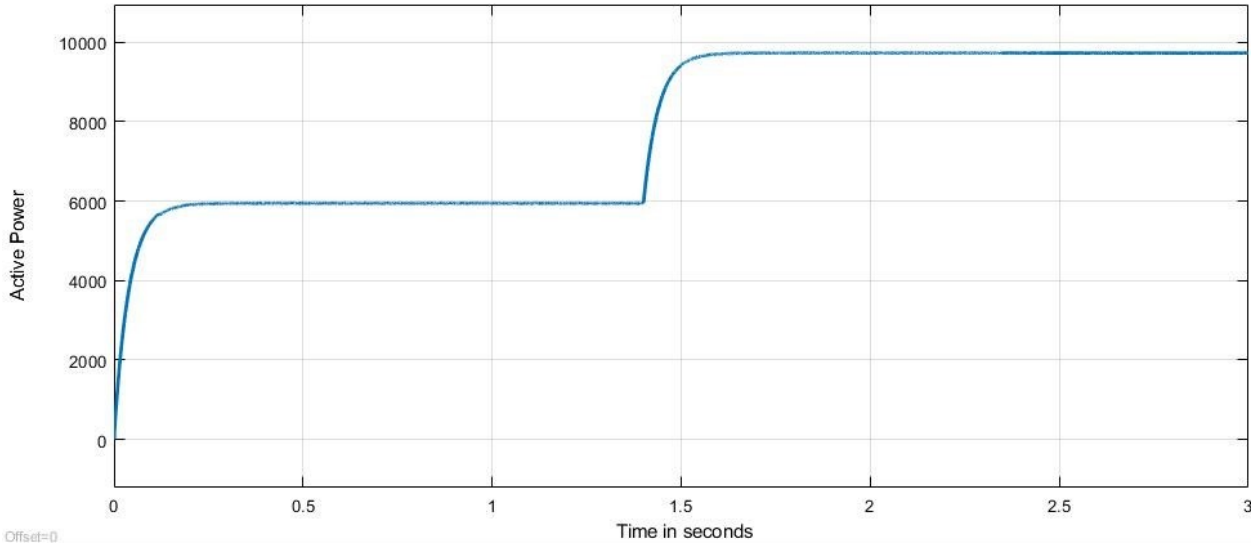

Fig. 4.7 Real power of VSG from light load to heavy load

4.4 Modeling and analysis of a VSG controller

The inverter with the additional governor is called the VSG. Table 4.2 shows the control parameters of VSG control. VSG has an improved droop characteristic and adds additional inertia in the system, and hence has a better control response than VSI and synchroverter as shown in figures 4.7 and 4.8. Even though primary control of VSG has satisfactory results, the output diverges due to oscillations caused by line reactance of large transmission lines. However under large transmission lines the performance of VSG deteriorates indicating a need for secondary controller.

4.5 Summary

The above work of mimicking the dynamic characteristics of a conventional synchronous generator helped us stabilize the output frequency and voltage. However, when operated in a multi-agent system, overall active and reactive power distribution is not a desirable way because of the static error drawback of VSG, especially when there is an unexpected load shifting. And, given the fact that VSG is also an inverter-based generator, the transient tolerance condition is much less than the synchronous generator. Consequently, VSG stops responding due to high oscillation caused

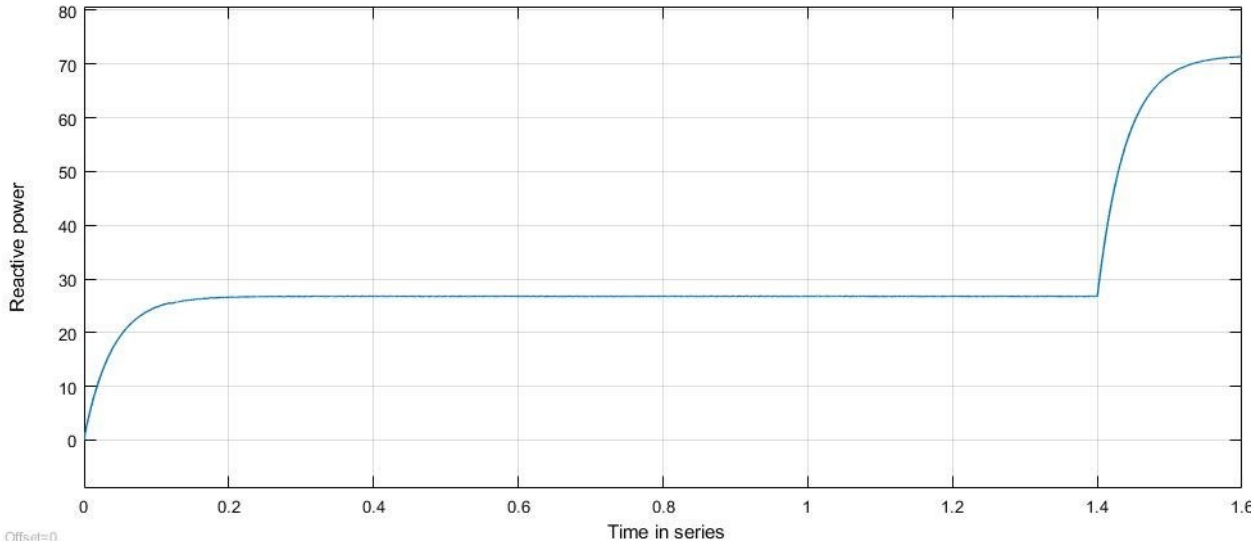

Fig. 4.8 Reactive power of VSG from light load to heavy load

by unexpected load shifting. To address these issues, the concept of VSG control improved and moved to hierarchical control.

CHAPTER 5

Consensus Based controller for Virtual Synchronous Generator

5.1 Introduction

The secondary control is designed for a VSG to compensate for the static effect and improve the power-sharing in DGs. In recent studies, consensus-based multi-agent control theory has been successfully applied for a decentralized control between the agents [31]. Considering DGs as agents the consensus algorithm is suitable for a decentralized control introducing additional communication and switching delays which are essential to the operation of VSG.

5.2 Graph theory and consensus algorithm

The consensus algorithm is well explained by Graph theory[31]. Consider a linear system $\dot{x} = Ax + Bu$ network is represented by a graph G (V, E) consists of the vertices V(x), and edges E(x). A graph that models asymmetrical relation, is called a directed graph and graph that is undirected, unweighted, and has fewer loops is called as a simple graph. All the units connected simple graph communicate with their neighbors to achieve consensus. Let A_G be the adjacent matrix of G(V,E),the off-diagonal element of A_G represent the communicative link of node i with node j. Entries of A_G, a_{ij}=a_{ji}=1 if edge set E (i, j) =1, i.e., node j is an element in vertex matrix and edge matrix, otherwise, a_{ij}=a_{ji}=0. Here,

$$\begin{aligned} a_{ij} = a_{ji} = 1 \ \ \forall \ \ E(i,j) = 1 \\ a_{ij} = a_{ji} = 0 \ \ \forall \ \ E(i,j) = 0 \end{aligned} \tag{5.1}$$

If L is the Laplacian of graph G then $L = D - A$, where D is the nxn degree matrix. The diagonal elements of the degree matrix represent edges of node i and all off diagonal adjacency matrix A is zero. The diagonal elements of laplacian matrix are given by 5.2 and graph G(V,E) with its dynamics $\dot{x}_i$=u_i is given by equation 5.6.

$$\begin{aligned} L_{ij} &= -a_{ij} \ \ \forall \ \ i \neq j \\ L_{ij} &= \sum(a_{ij}) \ \ \forall \ \ i = j \end{aligned} \tag{5.2}$$

Let incidence matrix $B = [b_1, b_2, b_3, ...b_m]$ of the graph with M distinct edges. The weighted laplacian is

$$L_w = BWB^T \tag{5.3}$$

where, $W = diag(w_1, w_2.....w_n)$ is edge weight matrix. The entries of incidence matrix are

$$\begin{aligned} B_{ij} &= 1 \ \ \forall \ \ i \text{ connected to } j \\ B_{ij} &= 0 \ \ \forall \ \ i \text{ not connected to } j \end{aligned} \tag{5.4}$$

5.3 Model Description

Consider a distributed network of microgrids connected through a weighted graph of G (V, E) with the nodes V, lines E and DGs are connected to V. Let the microgrid have N distributed generators and admittance matrix Y_{ij}.

$$Y_{ij} = G_{ij} + B_{ij} \tag{5.5}$$

Y_{ij}=0, if there is no connection between the nodes i and j. Under the steady-state condition, the active power and reactive power flow equations are:

$$\begin{aligned} P_i &= \sum_{j-1}^{n} V_i V_j (G_{ij} cos\theta_{ij} + B_{ij} sin\theta_{ij}) \\ Q_i &= \sum_{j-1}^{n} V_i V_j (G_{ij} sin\theta_{ij} - B_{ij} cos\theta_{ij}) \end{aligned} \tag{5.6}$$

In the above equation, P_i is the active power injection, $Q_i$is the reactive power injections to MG in each bus, B_{ij} is the susceptance of each transmission line, G_{ij} is the conductance of each transmission line. Let V_i and θ_i are the bus voltage magnitude and angle. The load dynamics are modeled using equation 5.7.

$$\begin{aligned} P_{Li} &= -P_i - D_{Lp,i}\dot{\theta}_i \\ Q_{Li} &= -Q_i - D_{Lq,i}\dot{V}_i \end{aligned} \tag{5.7}$$

It can be seen from equation 5.7, it can be concluded that the active power load is relatively insensitive to change in the voltage magnitude and the reactive power load is relatively insensitive to the change in the phase angle. Active power depends on bus frequency and reactive power depends on bus voltage and these dependencies are represented through $D_{Lp,i}$ and $D_{Lq,i}$ respectively.

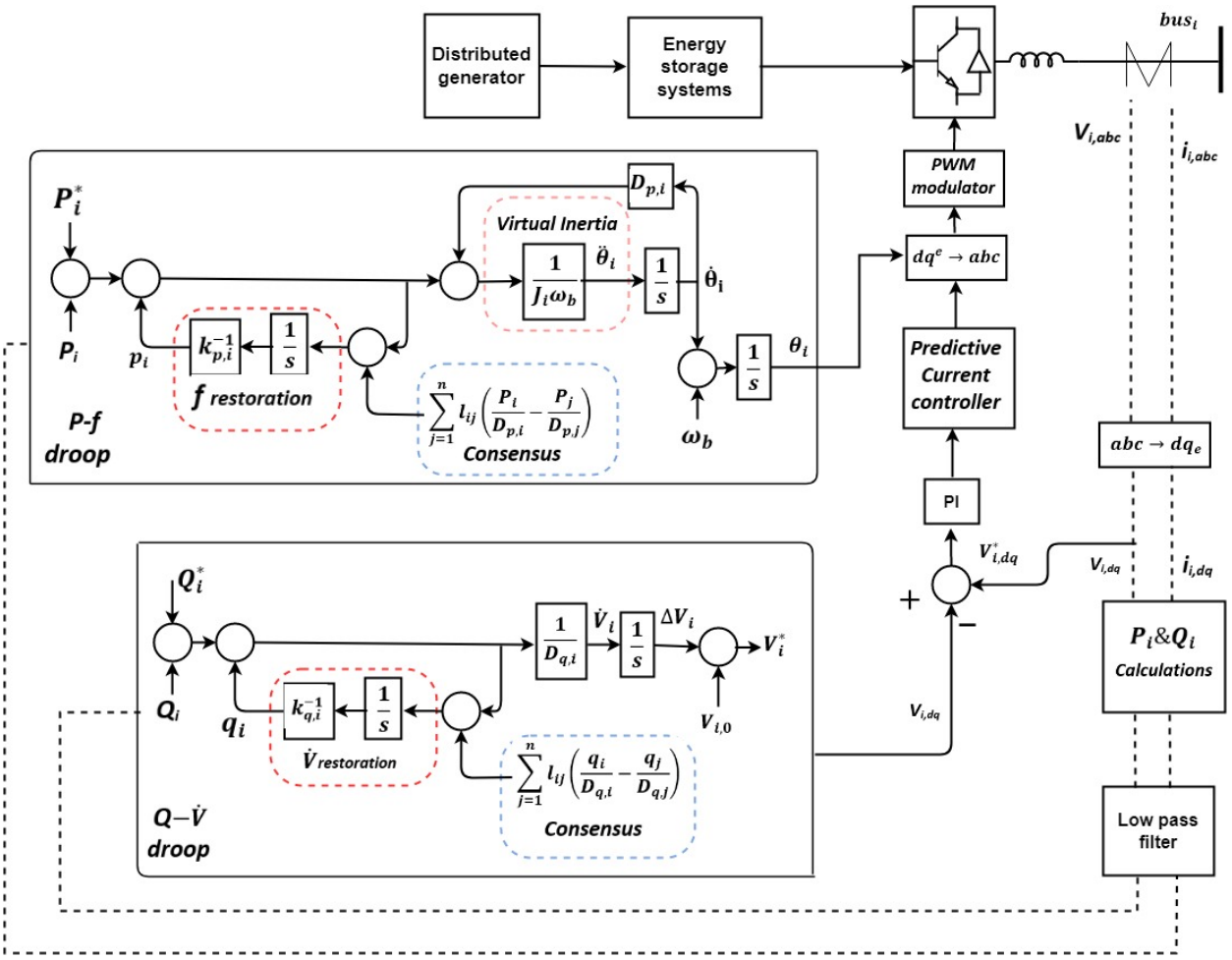

Fig. 5.1 Block diagram of consensus based virtual synchronous generator

5.4 Consensus-Based control of VSGs

Figure 5.1 shows the consensus controller with the detailed model of virtual synchronous generator that was developed in figure 3.8 that was developed. The power meter measures voltage and current which is used for calculating P_i and Q_i that act as reference for VSG control. This control has $P - f$ droop and $Q - V$ droop primary controllers with consensus based secondary controllers to regulate frequency and voltage. The outer control loop uses the θ and V from the consensus based controller and generates PWM signals. The consensus-based VSG control uses data exchanged between neighbors for real and reactive power-sharing. A second-order differential equation and hence the consensus controller designed is also second order. However, the reactive power control remains unchanged. The control block diagram of VSG is illustrated in Figure 5.1 and the closed-

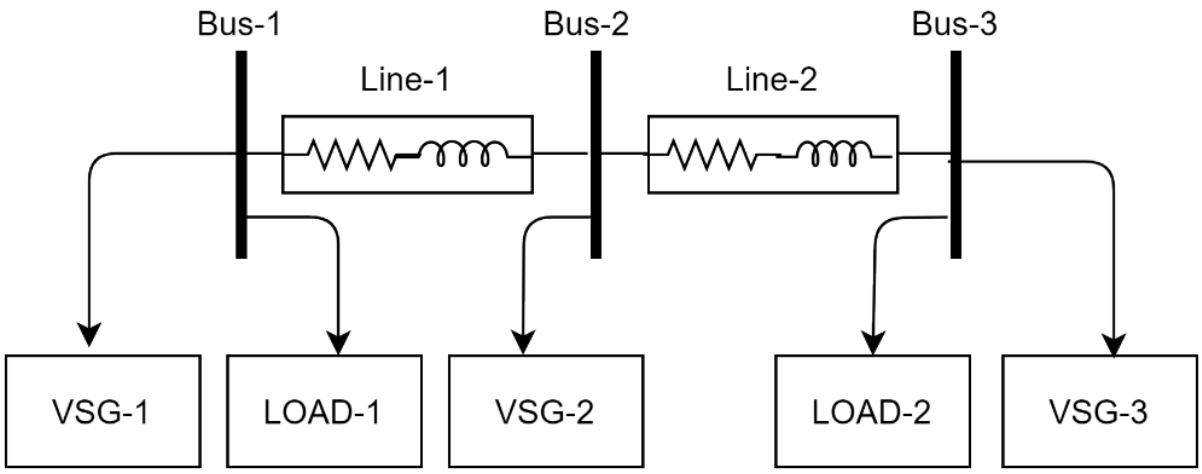

Fig. 5.2 Single line diagram of microgrid

loop consensus-based VSG equations as described in 5.8.

$$\begin{aligned}
\dot{\theta}_i &= \omega_i - \omega_b \\
J_i\omega_b\omega_i + D_{p,i}\dot{\theta}_i &= P_i^* - P_i - p_i \\
k_{p,i}\dot{p}_i &= P_i^* - P_i - p_i + \sum_{j=1}^{m} l_{ij}\Big(\frac{p_i}{D_{p,i}} - \frac{p_j}{D_{p,j}}\Big) \\
D_{q,i}V_i\dot{v}_i &= Q_i^2 - Q_i - q_i \\
k_{q,i}\dot{q}_i &= Q_i^* - Q_i - q_i + \sum_{j=1}^{m} l_{ij}\Big(\frac{q_i}{D_{q,i}} - \frac{q_j}{D_{q,j}}\Big)
\end{aligned} \tag{5.8}$$

Here $D_{p,i}$ and $D_{q,i}$ are the droop gains for active and reactive power control, P_i^* and Q_i^* are nominal power ratings and the transformed bus voltage $\dot{v}_i = \dot{V}_i V_i^{-1}$. The p_i and q_i are first-order control actions which describe the $\dot{\theta}_i$ and $\dot{V}_i$ restoration mechanism for regulating frequency variable and voltage magnitude. Restoration rates are $k_{p,i}^{-1}D_{p,i}$ and $k_{q,i}^{-1}D_{q,i}$ respectively. The physical connectivity between the vertices of the network are represented by L_comm, where each element l_{ij} represents a communication link between DG_i and DG_j.

5.5 Simulations and Results Demonstration

To validate the performance of consensus-based frequency and voltage droop control of VSG, a simulation of 3-bus and 3 DG microgrid is implemented, as shown in the Figure 5.2. The simulation is modeled using MATLAB/Simulink using the parameters in Table 5.1. The phase angle and

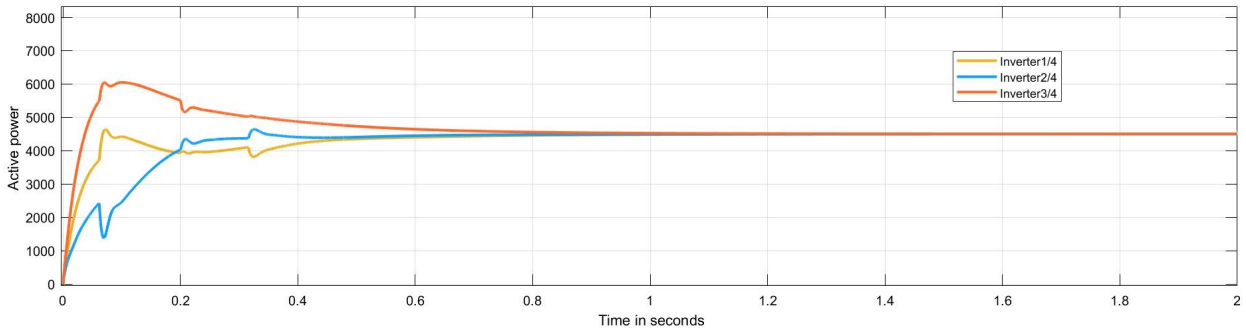

Fig. 5.3 Real power sharing among consensus VSGs

the magnitude for inner loop voltage controllers are determined through droop controllers.

Table 5.1 System parameters

parameters	values	parameters	values
$1/D_{p,i}$	0.00002	$Load_1$	25
j_i	1.061	$Load_2$	20
$1/D_{p,j}$	0.006	$line_1$	[0.23,0.1]
$k_{p,i}$	0.001	$line_2$	[0.35,0.58]
$k_{q,i}$	0.001	$Inverter\ \ rating$	10kVA
$L_{com,p}$	0.000001	$L_{com,q}$	0.0001

5.6 Simulation results

Figure 5.2 shows microgrid system whose nominal frequency is 50Hz and operates at 220v with loads modeled as constant impedance. Five scenarios are considered where the first three scenarios consider load change where fourth and fifth consider line impedance changes.

5.6.1 Case-1: Power sharing for resistive loads

In the first scenario only resistive loads are considered. Figures 5.3 and5.4 show real and reactive power of the DGs and it is seen that reactive power generated by DG_1 and DG_3 is absorbed by DG_2 so that the reactive power output is zero.

5.6.2 Case -2: Consensus based power sharing for change in resistive load

Consider an increase in load on bus-1 at 2 seconds. Figure 5.5 and 5.6 shows that the DGs adjust the real and reactive power with in 0.3seconds when load increases at 2seconds. Reactive power generated remains at zero.

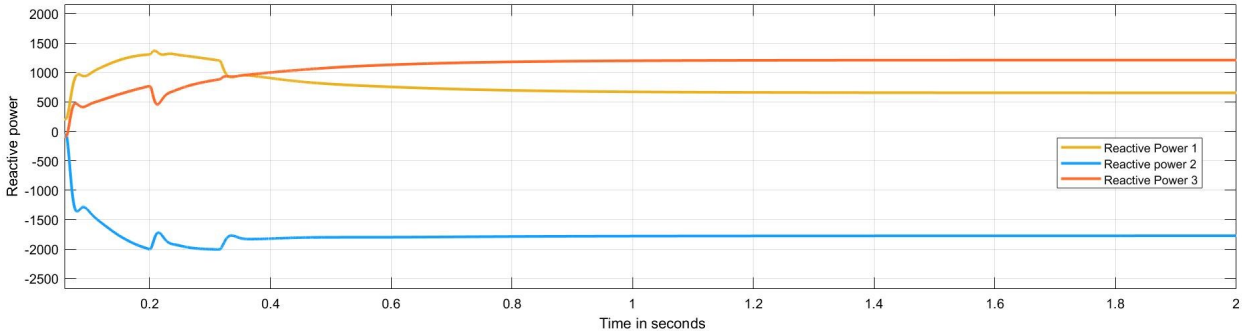

Fig. 5.4 Reactive power sharing among consensus VSGs

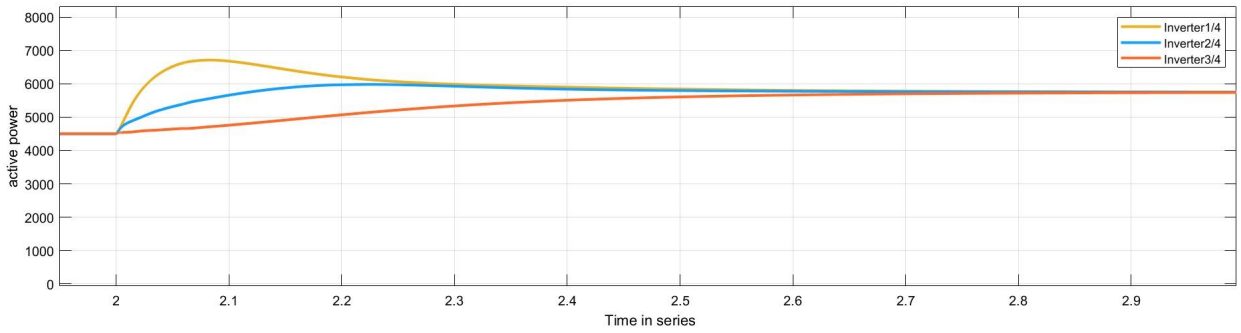

Fig. 5.5 Real power sharing among consensus VSGs at load change

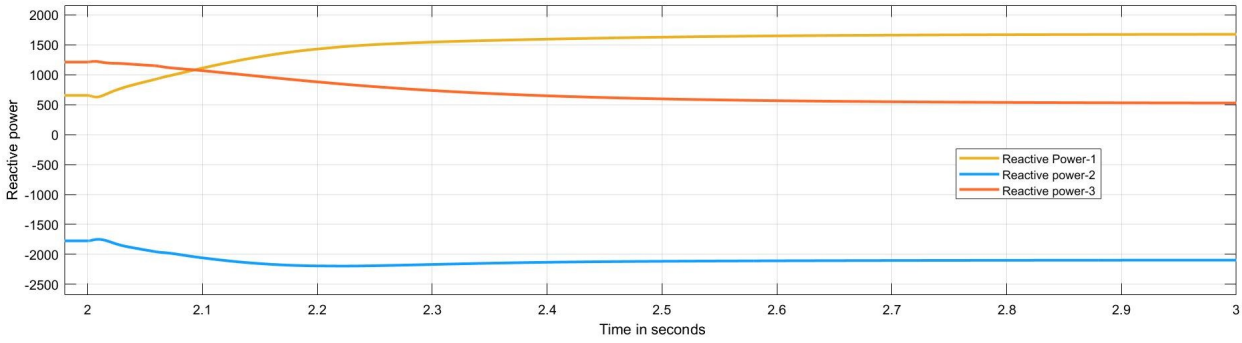

Fig. 5.6 Reactive power sharing among consensus VSGs at load change

5.6.3 Case-3: Consensus-based power-sharing for inductive loads

The reactive power sharing among the DGs can be represented by taking RL-loads. Consider a inductive load at bus-1 and a resistive load at bus-3. Figure 5.7 and 5.8 shows that the DGs adjust the real and reactive power with in 0.5 seconds when load increases at 2 seconds representing the fast settling time.

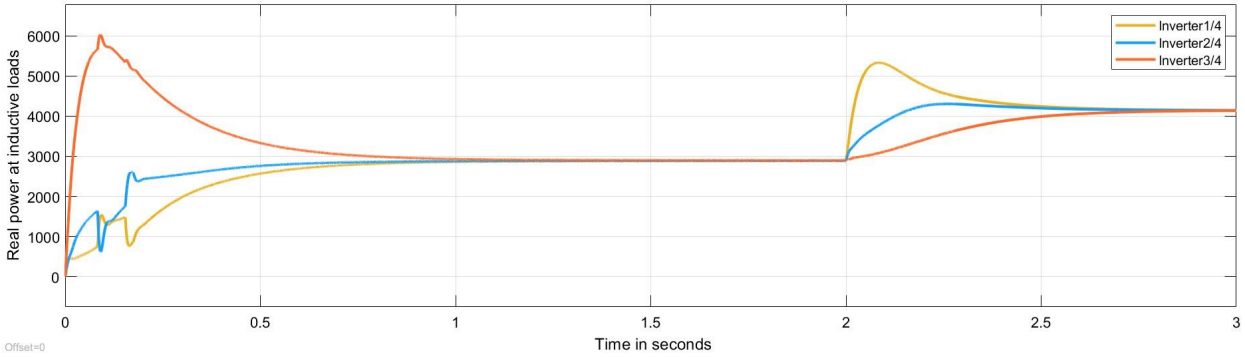

Fig. 5.7 Real power sharing among consensus VSGs with inductive loads

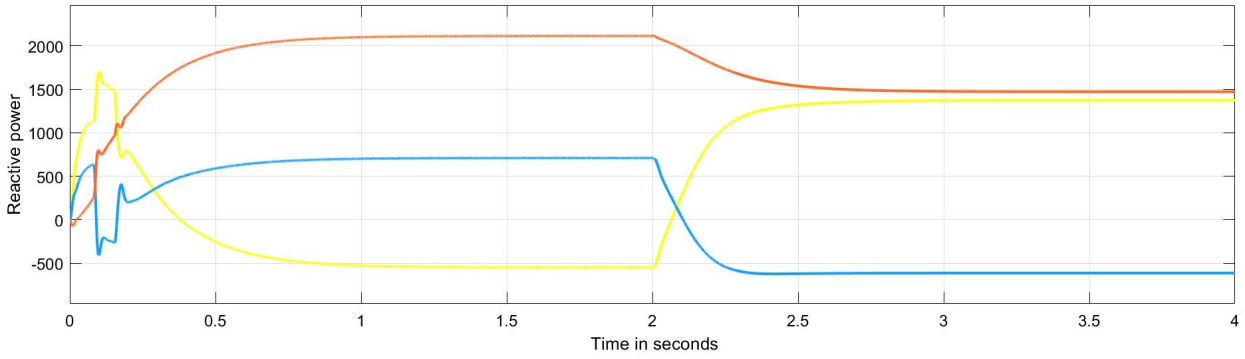

Fig. 5.8 Reactive power sharing among consensus VSGs with inductive loads

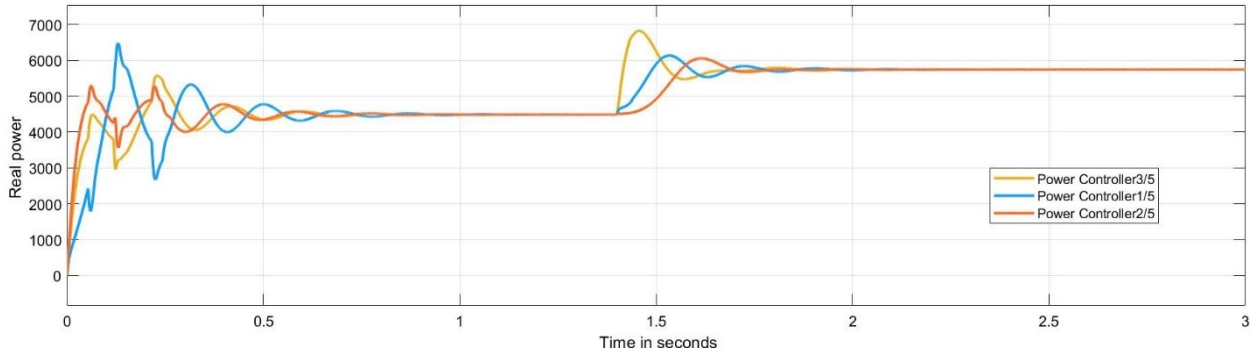

Fig. 5.9 Real power sharing among VSGs

5.6.4 Case-4: Power sharing for change in R-L load

Consider a inductive load at bus-1 and a resistive load at bus-3. By comparing Figures 5.9 and 5.10 with figures 5.7 and 5.8 it can be seen that consensus based algorithm improves the controller response by improving the settling time and reducing oscillations.

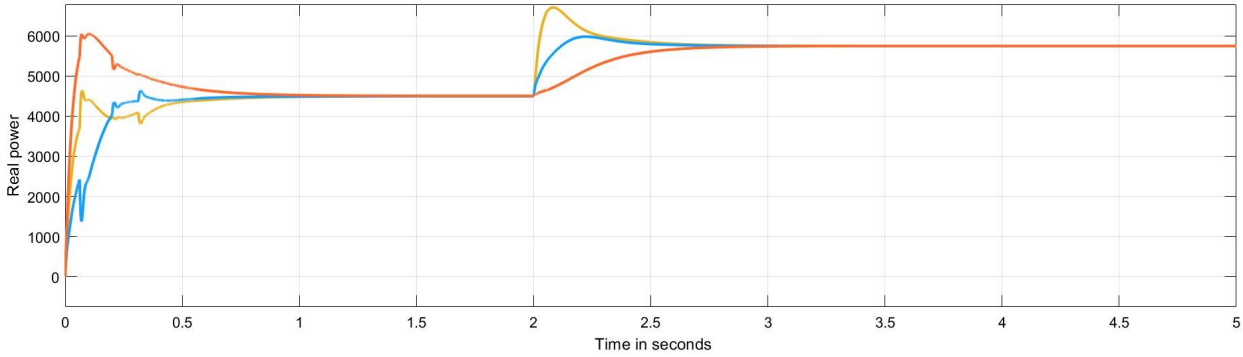

Fig. 5.10 Real power sharing among consensus VSGs

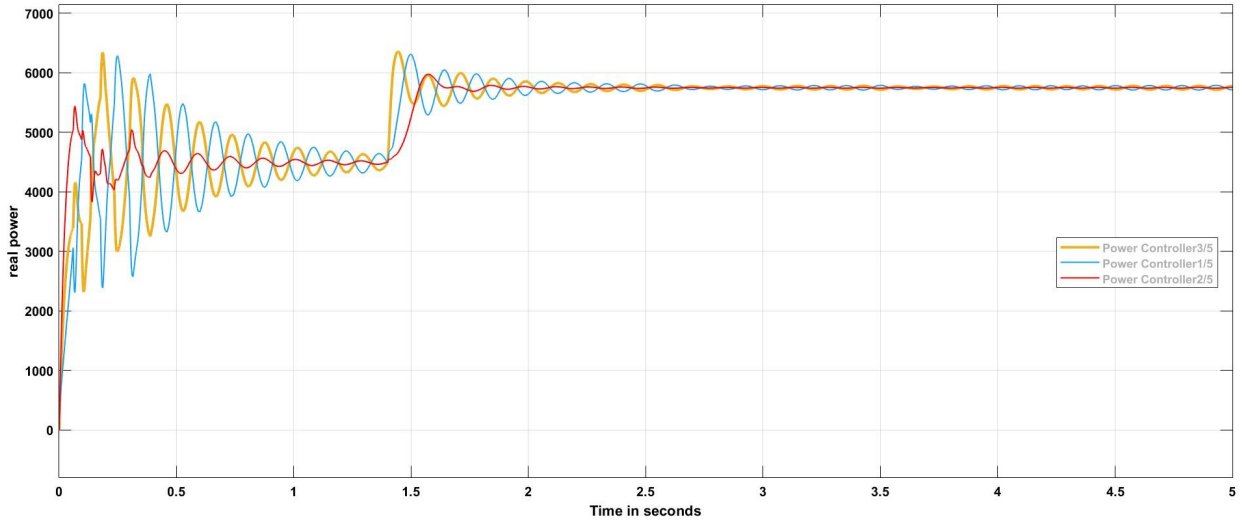

Fig. 5.11 Real power sharing among VSGs with change in line impedance

5.6.5 Case study-5: Power sharing for change in R-L load and r/x ratio

Consider a change in R/X ratio of the line between bus-1 and bus-2. Figures 5.11 and 5.12 that the DGs tuned the real and reactive power sharing when their is load change. And also the consensus-based algorithm improves the controller response with the impact of change in line impedance by improving the settling time and reducing oscillations.

5.7 Summary

The proposed controller mechanism of VSG is governed by the second-order swing equation with the nonzero moment of inertia and damping mechanism. Therefore, frequency deviations are reduced. Furthermore, since the consensus-based VSG has a conventional decentralized droop design, the real and reactive power mismatch has a distributed averaging proportional-integral con-

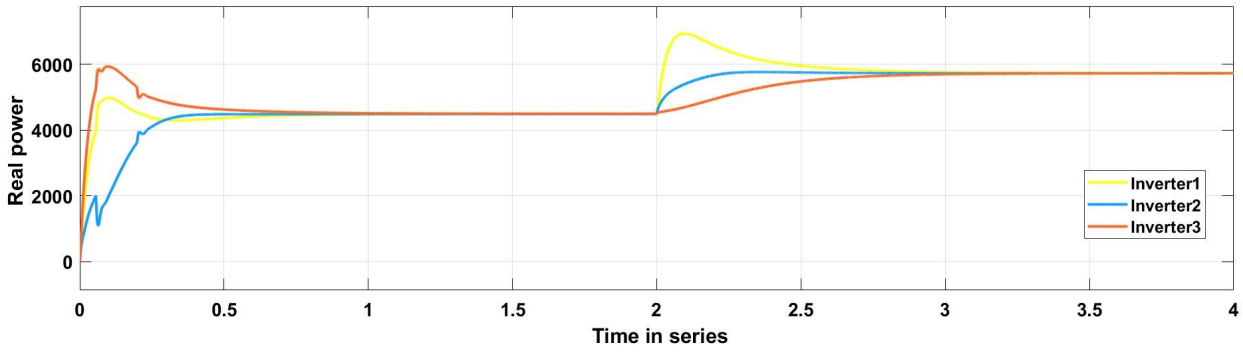

Fig. 5.12 Real power sharing among consensus VSGs with change in line impedance

trol.

CHAPTER 6

Conclusion and Future Work

6.1 Conclusion

The research work presented in this thesis has focused on the microgrid challenges when renewable energy sources dominate the microgrid. An account of the main contributions is given as follows:

- The implementation of virtual inertia through synchronverters and virtual synchronous generator were studied.
- The overall dynamics of VSG presented in the thesis have implemented virtual inertia effectively in the system based on the given microgrid nature.
- It has also verified that the consensus algorithm can regulate the frequency and voltage of multiple VSGs near their rated values, with appropriate power-sharing by very sparse communication. The fastest response with the highest connectivity level between the distributed generators is achieved. The looped topology in the consensus algorithm gave us the fastest response and improved the efficiency of the microgrid.
- The effect of line impedances on grid stability is also examined in the thesis through a consensus algorithm. The result shows that the consensus algorithm restores the system dynamics without any parameter changes.

6.2 Future work

- This study can be further explored and be made even more realistic by including communication complexities like different communication delays.
- Fault analysis should also be done in this control scheme because the generator works based on consensus feedback, theoretically increasing the electrical fault levels. Therefore, the protection of microgrids should also be adequately studied so that the electrical system can sustain and isolate any fault without significant damages.

- A small-signal analysis should be done to study the proper influence of all the parameters used in a higher-order system.
- To see the real-world challenges, the effectiveness of the controller should be tested in microgrid clusters, and the implementation the solar or wind renewables in the system can be considered.
- A Hardware-in-the-Loop (HILP) can be implemented, which can mimic the response of the entire power system.
- The grid dominated by virtual inertia units, the aggregated operation, and optimal placement can be important research topics.
- The virtual inertia control efficiency should be studied by considering HVAC links.
- The wide adoption and integration of technological innovations like data-driven techniques open a wide area of research in the control of microgrids.
- The constant change of system inertia and system dynamics in the system with a high share of RESs, real-time synchronized measurement data, such as the data obtained from phasor measurement units (PMUs), should be considered and estimated inertia requirements can be studied.

LIST OF PUBLICATIONS

1. **A. Kandula**, V. Verma, S. K. Solanki, and J. Solanki, ”Comparative Analysis of Self-Synchronized Virtual Synchronous Generator Control and Droop Control for Inverters in Islanded Microgrid,” in North American Power Symposium (NAPS), 2019.

Bibliography

[1] A Salehi Dobakhshari, Salehi Azizi, and AM Ranjbar. “Control of microgrids: Aspects and prospects”. In: *2011 International Conference on Networking, Sensing and Control*. IEEE. 2011, pp. 38–43.

[2] “US Energy Report”. In: (2018).

[3] Yeliz Yoldaş et al. “Enhancing smart grid with microgrids: Challenges and opportunities”. In: *Renewable and Sustainable Energy Reviews* 72 (2017), pp. 205–214.

[4] Nagaraju Pogaku, Milan Prodanovic, and Timothy C Green. “Modeling, analysis and testing of autonomous operation of an inverter-based microgrid”. In: *IEEE Transactions on power electronics* 22.2 (2007), pp. 613–625.

[5] Qing-Chang Zhong and George Weiss. “Synchronverters: Inverters that mimic synchronous generators”. In: *IEEE transactions on industrial electronics* 58.4 (2010), pp. 1259–1267.

[6] Josep M Guerrero et al. “Hierarchical control of droop-controlled AC and DC microgrids—A general approach toward standardization”. In: *IEEE Transactions on industrial electronics* 58.1 (2010), pp. 158–172.

[7] Ali Bidram and Ali Davoudi. “Hierarchical structure of microgrids control system”. In: *IEEE Transactions on Smart Grid* 3.4 (2012), pp. 1963–1976.

[8] Tine L Vandoorn et al. “A control strategy for islanded microgrids with dc-link voltage control”. In: *IEEE Transactions on Power Delivery* 26.2 (2011), pp. 703–713.

[9] Juan C Vasquez et al. “Modeling, analysis, and design of stationary-reference-frame droop-controlled parallel three-phase voltage source inverters”. In: *IEEE Transactions on industrial electronics* 60.4 (2012), pp. 1271–1280.

[10] Qing-Chang Zhong. “Robust droop controller for accurate proportional load sharing among inverters operated in parallel”. In: *IEEE Transactions on industrial Electronics* 60.4 (2011), pp. 1281–1290.

[11] Hassan Bevrani, Toshifumi Ise, and Yushi Miura. “Virtual synchronous generators: A survey and new perspectives”. In: *International Journal of Electrical Power and Energy Systems* 54 (2014), pp. 244–254.

[12] Salvatore D'Arco, Jon Are Suul, and Olav B Fosso. "A Virtual Synchronous Machine implementation for distributed control of power converters in SmartGrids". In: *Electric Power Systems Research* 122 (2015), pp. 180–197.

[13] Zishun Peng et al. "Virtual synchronous generator control strategy incorporating improved governor control and coupling compensation for AC microgrid". In: *IET Power Electronics* 12.6 (2019), pp. 1455–1461.

[14] Jingyang Fang et al. "A battery/ultracapacitor hybrid energy storage system for implementing the power management of virtual synchronous generators". In: *IEEE Transactions on Power Electronics* 33.4 (2017), pp. 2820–2824.

[15] Jia Liu, Yushi Miura, and Toshifumi Ise. "Comparison of dynamic characteristics between virtual synchronous generator and droop control in inverter-based distributed generators". In: *IEEE Transactions on Power Electronics* 31.5 (2015), pp. 3600–3611.

[16] Jia Liu et al. "Parallel operation of a synchronous generator and a virtual synchronous generator under unbalanced loading condition in microgrids". In: *2016 IEEE 8th International Power Electronics and Motion Control Conference (IPEMC-ECCE Asia)*. IEEE. 2016, pp. 3741–3748.

[17] Xiangwu Yan et al. "Parallel operation of virtual synchronous generators and synchronous generators in a microgrid". In: *The Journal of Engineering* 2019.16 (2019), pp. 2635–2642.

[18] Jaber Alipoor, Yushi Miura, and Toshifumi Ise. "Power system stabilization using virtual synchronous generator with alternating moment of inertia". In: *IEEE journal of Emerging and selected topics in power electronics* 3.2 (2014), pp. 451–458.

[19] Xin Meng et al. "A new master-slave based secondary control method for virtual synchronous generator". In: *2016 IEEE 2nd Annual Southern Power Electronics Conference (SPEC)*. IEEE. 2016, pp. 1–6.

[20] Gang Yao et al. "A virtual synchronous generator based hierarchical control scheme of distributed generation systems". In: *Energies* 10.12 (2017), p. 2049.

[21] Kun Jiang, Hongsheng Su, and Ding Sun. "Secondary frequency regulation scheme based on improved virtual synchronous generator in an islanded microgrid". In: *Journal of Vibroengineering* 21.1 (2019), pp. 215–227.

[22] Lin-Yu Lu and Chia-Chi Chu. "Robust consensus-based droop control for multiple power converters in isolated micro-grids". In: *2014 IEEE International Symposium on Circuits and Systems (ISCAS)*. IEEE. 2014, pp. 1820–1823.

[23] Deepak Tiwari et al. "Vehicle-to-Grid Integration for Enhancement of Grid: A Distributed Resource Allocation Approach". In: *IEEE Access* 8 (2020), pp. 175948–175957.

[24] Lin-Yu Lu and Chia-Chi Chu. “Consensus-based secondary frequency and voltage droop control of virtual synchronous generators for isolated AC micro-grids”. In: *IEEE Journal on Emerging and Selected Topics in Circuits and Systems* 5.3 (2015), pp. 443–455.

[25] Lingling Fan. *Control and dynamics in power systems and microgrids*. CRC Press, 2017.

[26] Prabha Kundur. “Power system stability”. In: *Power system stability and control* (2007), pp. 7–1.

[27] Ujjwol Tamrakar et al. “Virtual inertia: Current trends and future directions”. In: *Applied Sciences* 7.7 (2017), p. 654.